

DESIGN, CONSTRUCTION AND PERFORMANCE EVALUATION OF A  
CONSTANT AIR VOLUME DEVICE FOR HVAC SYSTEMS

A THESIS SUBMITTED TO  
THE GRADUATE SCHOOL OF NATURAL AND APPLIED SCIENCES  
OF  
MIDDLE EAST TECHNICAL UNIVERSITY

BY

CANER EKİN KİPER

IN PARTIAL FULFILLMENT OF THE REQUIREMENTS  
FOR  
THE DEGREE OF MASTER OF SCIENCE  
IN  
MECHANICAL ENGINEERING

FEBRUARY 2018



Approval of the thesis:

**DESIGN, CONSTRUCTION AND PERFORMANCE EVALUATION OF A  
CONSTANT AIR VOLUME DEVICE FOR HVAC SYSTEMS**

submitted by **CANER EKİN KİPER** in partial fulfillment of the requirements for the degree of **Master of Science in Mechanical Engineering Department, Middle East Technical University** by,

Prof. Dr. Gülbin Dural Ünver  
Dean, Graduate School of **Natural and Applied Sciences**

\_\_\_\_\_

Prof. Dr. M.A.Sahir Arıkan  
Head of Department, **Mechanical Engineering**

\_\_\_\_\_

Prof. Dr. Kahraman Albayrak  
Supervisor, **Mechanical Engineering Department, METU**

\_\_\_\_\_

**Examining Committee Members:**

Assoc. Prof. Dr. Cüneyt Sert  
Mechanical Engineering Department, METU

\_\_\_\_\_

Prof. Dr. Kahraman Albayrak  
Mechanical Engineering Department, METU

\_\_\_\_\_

Assoc. Prof. Dr. M. Metin Yavuz  
Mechanical Engineering Department, METU

\_\_\_\_\_

Assist. Prof. Dr. Özgür Bayer  
Mechanical Engineering Department, METU

\_\_\_\_\_

Prof. Dr. Selin Aradağ Çelebioğlu  
Mechanical Engineering Department, TOBB ETU

\_\_\_\_\_

**Date:**

\_\_\_\_\_

**I hereby declare that all information in this document has been obtained and presented in accordance with academic rules and ethical conduct. I also declare that, as required by these rules and conduct, I have fully cited and referenced all material and results that are not original to this work.**

Name, Last Name: CANER EKİN KİPER

Signature :

## **ABSTRACT**

### **DESIGN, CONSTRUCTION AND PERFORMANCE EVALUATION OF A CONSTANT AIR VOLUME DEVICE FOR HVAC SYSTEMS**

Kiper, Caner Ekin

M.S., Department of Mechanical Engineering

Supervisor : Prof. Dr. Kahraman Albayrak

February 2018, 89 pages

Everything that is used by humans in daily life is designed to increase the quality of life of people. This shows that comfort may be the last thing human beings are willing to give up. Heating, Ventilating and Air Conditioning (HVAC) systems are also designed to increase life standards in enclosed environments such as meeting rooms, offices, concert halls etc. People feel more comfortable when the ventilation system and ambient temperature is set properly. However, in some situations, setting the operating conditions to the right value is not an easy task. This might require a more detailed analysis employing different type of ventilating methods. Sometimes combining various methods could be a solution or even designing a completely new system that satisfies the need of the people may be necessary.

This thesis aims to provide a design and test procedure for constant air volume (CAV) device for Heating Ventilating and Air Conditioning (HVAC) systems. CAV unit closely resembles a butterfly valve. Pressure loss and moment characterization ac-

ording to blade angles are obtained by means of several experiments and numerical studies. These experiments are explained in detail. Obtained data from experiments are compared to validate CFD analysis results. The CAV unit supplies constant air flow rate even if differential pressure over the unit changes. In order to obtain a constant air flow rate, a control mechanism is proposed and details of it is given.

**Keywords:** CAV Unit, CFD analysis, HVAC, Constant Air Volume, Butterfly Valve

## ÖZ

### **HAVALANDIRMA SİSTEMLERİ İÇİN SABİT HAVA DEBİSİ AYAR ÜNİTESİ TASARIMI KONSTRÜKSİYONU VE PERFORMANS DEĞERLENDİRMESİ**

Kiper, Caner Ekin

Yüksek Lisans, Makina Mühendisliği Bölümü

Tez Yöneticisi : Prof. Dr. Kahraman Albayrak

Şubat 2018, 89 sayfa

İnsanların günlük hayatlarında kullandığı her şey onların rahatını artırmak amacıyla tasarlanmıştır. Bu da gösteriyor ki insanoğlunun vazgeçeceği en son şey belki de kendi rahatıdır. Havalandırma sistemleri de insanların toplantı odalarında, ofislerde ve konser salonları gibi yerlerde rahatını artırmak amacıyla tasarlanmıştır. Havalandırma miktarı ve ortamın sıcaklık değeri doğru bir şekilde ayarlandığında insanlar kendilerini rahatta hissederler. Fakat bazı durumlarda uygun çalışma koşullarını belirlemek pek kolay olmayabilir. Detaylı analizlerin yapılması, farklı havalandırma ve iklimlendirme yöntemlerinin kullanılması gerekebilir veya ihtiyaçları karşılayan yeni bir havalandırma ekipmanının tasarlanması gerekli olabilir.

Bu tezin amacı iklimlendirme sistemlerinde kullanılacak olan sabit hava debisi ayar ünitesi tasarımı ve test yöntemleri hakkında bilgi sağlamaktır. Sabit hava debisi ayar ünitesinin kelebek vanaya oldukça benzeyen bir yapısı vardır. Basınç kaybı ve tork ka-

rakterizasyonu ünite kanadı açısına göre laboratuvar deneyleri ve sayısal deneylerle yapılmıştır. Bu deneylerin ayrıntıları tez içerisinde verilmiştir. Elde edilen HAD analizi sonuçları, laboratuvar deneylerinin sonuçları ile karşılaştırılarak HAD analizleri doğrulanmıştır. Sabit hava debisi ayar ünitesi, hava debisini ünite üzerindeki basınç düşüşü değişse de sabit tutar. Hava debisini sabit tutabilmek için bir kontrol mekanizması önerilmiştir ve mekanizmanın detayları tez içerisinde verilmiştir.

Anahtar Kelimeler: CAV Kutu, HAD Analizi, İklimlendirme Sistemleri, Sabit Hava Debisi, Kelebek Vana



*dedicated to my family*

## ACKNOWLEDGMENTS

I would like to thank my thesis supervisor Prof. Dr. Kahraman ALBAYRAK, for his guidance, support, deep patience throughout my study.

I can never forget the support of my parents Şerife Kiper, Menderes Kiper and my sister Evrim Yağmur Kiper. Without their belief, this study can not be completed.

I wish to express my deepest gratitude to my love Büşra Taş for her belief and encouragement during this study.

This thesis is mainly supported by a TÜBİTAK TEYDEB 1507 project which is proposed by Kes Klima. I would like to thank Mr. Ali Can Güven, head of manufacturing department, Mr. Korkut VAROL, head of Research and Development Department, Mr. Onur ARSLAN, vice general manager, and Mr. Hakan KES, general manager, for their advices, financial support throughout the thesis. I also thank all of the Kes Klima workers who help me during my thesis.

## TABLE OF CONTENTS

ABSTRACT . . . . .	v
ÖZ . . . . .	vii
ACKNOWLEDGMENTS . . . . .	x
TABLE OF CONTENTS . . . . .	xi
LIST OF TABLES . . . . .	xvi
LIST OF FIGURES . . . . .	xvii
LIST OF ABBREVIATIONS . . . . .	xxii
CHAPTERS	
1 INTRODUCTION . . . . .	1
1.1 General Information on HVAC Systems . . . . .	3
1.1.1 All Water Systems . . . . .	3
1.1.2 Air - Water Systems . . . . .	3
1.1.3 All Air Systems . . . . .	3

1.1.3.1	Dual-Duct System . . . . .	4
1.1.3.2	Variable Air Volume Systems (VAV) . . . . .	4
1.1.3.3	Single - Zone System . . . . .	6
1.2	General Information on Typical Fan System and Operating Principle of CAV Unit . . . . .	7
1.2.1	Controlling Volumetric Flow Rate of a Fan . . . . .	8
1.2.2	Operating Principle of CAV Unit . . . . .	9
1.3	Literature Survey . . . . .	10
1.4	Objectives and Outline of the Thesis . . . . .	13
2	DESIGN OF THE CONSTANT AIR VOLUME UNIT . . . . .	15
2.1	Design Goals, Limitations and Strategy . . . . .	15
2.2	Examination of a CAV Unit, Benchmark Tests and Results . . . . .	16
2.2.1	Commercial CAV Unit and Components . . . . .	17
2.2.1.1	Blade of CAV Unit . . . . .	17
2.2.1.2	Control Box of CAV Unit . . . . .	18
2.2.2	Benchmark Tests and Results . . . . .	19
2.3	Design of CAV Unit . . . . .	23
2.3.1	Operating Characteristics of CAV Unit . . . . .	24

2.3.2	Calculation of Pressure Drop and Moment on the CAV Unit Blade . . . . .	26
2.3.3	Mathematical Relations between Torque on The Blade and Extension of Tension Spring . . . . .	30
2.3.4	Tension Spring Selection . . . . .	33
2.4	CAD Model of CAV Unit . . . . .	34
2.4.1	CAV Unit Components . . . . .	35
2.4.1.1	Air duct (Case) . . . . .	35
2.4.1.2	CAV Unit (Damper) Blade . . . . .	35
2.4.1.3	Control Box . . . . .	36
3	CFD ANALYSES OF CONSTANT AIR VOLUME (CAV) UNIT . . .	39
3.1	General Information and CFD Integration . . . . .	39
3.2	CFD Analyses . . . . .	40
3.2.1	Simplified CAV Unit Geometry . . . . .	40
3.2.2	Meshing . . . . .	41
3.2.3	Boundary Conditions . . . . .	43
3.3	CFD Analyses Results . . . . .	44
3.3.1	Comparison of Theoretical and CFD Results . . . .	48

4	EXPERIMENTAL FACILITIES AND PERFORMANCE EVALUATIONS . . . . .	53
4.1	Test Setup . . . . .	54
4.2	Calibration of Test Instruments . . . . .	57
4.3	Uncertainty Analysis . . . . .	58
4.4	Laboratory Measurements . . . . .	59
4.4.1	Pressure Drop Measurement . . . . .	59
	4.4.1.1 Pressure Drop Measurement Procedure	60
4.4.2	Bellows Pressure Measurement . . . . .	61
4.4.3	Measurement of Moment on the CAV Unit Blade . . . . .	62
	4.4.3.1 Moment Measurement Procedure . . . . .	65
4.4.4	Spring Constant Measurement . . . . .	65
	4.4.4.1 Spring Constant Measurement Procedure . . . . .	66
4.4.5	Air Velocity Measurement . . . . .	66
4.5	Laboratory Measurements Results . . . . .	67
4.5.1	Pressure Measurement Results . . . . .	68
	4.5.1.1 Bellows Pressure Measurement Results	69
4.5.2	Moment Measurement Results . . . . .	70

4.5.3	Spring Constant Measurement Results . . . . .	71
4.5.4	Air Velocity Measurement . . . . .	72
4.6	Discussions for Laboratory Measurements . . . . .	72
4.7	Performance Evaluations of CAV Unit . . . . .	73
5	DISCUSSION AND CONCLUSION . . . . .	75
5.1	Discussion . . . . .	75
5.2	Conclusion . . . . .	79
	REFERENCES . . . . .	81
APPENDICES		
A	PERFORMANCE EVALUATION OF Ø160 MM CAV UNIT . . . . .	85
B	FINAL VERSION OF CAV UNIT . . . . .	89

## LIST OF TABLES

### TABLES

Table 2.1	Air Flow Rate Ranges and Re Numbers for Ø160 mm CAV Unit . . .	23
Table 2.2	Contraction Coefficients . . . . .	27
Table 3.1	Deviation between Eqn 2.2 and CFD Results . . . . .	49
Table 3.2	Deviation Between Eqn 2.7 and CFD Results . . . . .	50
Table 3.3	Deviation Between Spring Moment and CFD Results . . . . .	51
Table 4.1	Spring Constants . . . . .	71



## LIST OF FIGURES

### FIGURES

Figure 1.1 Typical CAV Unit . . . . .	2
Figure 1.2 Schematic of All Air HVAC System . . . . .	4
Figure 1.3 VAV System . . . . .	5
Figure 1.4 VAV Box . . . . .	5
Figure 1.5 CAV System and CAV Unit . . . . .	6
Figure 1.6 Mechanical CAV Unit . . . . .	7
Figure 1.7 System Curve, Fan Curve and Operating Point . . . . .	8
Figure 1.8 Change in System Curve with Throttling . . . . .	9
Figure 1.9 Venturi Shape CAV Unit . . . . .	10
Figure 1.10 Operating Principle of a Venturi Type CAV Unit . . . . .	10
Figure 1.11 Flow Chart of CAV Unit Design . . . . .	14
Figure 2.1 Commercially Available CAV Unit . . . . .	17
Figure 2.2 CAV Unit Blade . . . . .	18
Figure 2.3 Assembly of Piston . . . . .	18
Figure 2.4 Control Box for CAV Unit . . . . .	19

Figure 2.5	Benchmark Test Results for 200 mm Diameter CAV Unit for $\pm 500m^3/h$	20
Figure 2.6	Benchmark Test Results for 200 mm Diameter CAV Unit for $\pm 800m^3/h$	20
Figure 2.7	Benchmark Test Results for 200 mm Diameter CAV Unit for $\pm 500m^3/h$	21
Figure 2.8	Benchmark Test Results for 200 mm Diameter CAV Unit for $\pm 700m^3/h$	21
Figure 2.9	Typical fan curve and system resistance curve . . . . .	24
Figure 2.10	Schematics of CAV Unit . . . . .	25
Figure 2.11	2D Model of CAV Unit . . . . .	26
Figure 2.12	Jet Velocity According to Blade Angle . . . . .	28
Figure 2.13	Calculated Pressure Drop According to Blade Angle . . . . .	28
Figure 2.14	Calculated Torque According to Blade Angle . . . . .	29
Figure 2.15	CAV Unit (unstretched and stretched spring position) . . . . .	30
Figure 2.16	Calculated Spring Constant Blade vs Blade Angle . . . . .	31
Figure 2.17	Comparison of Calculated Aerodynamic Torque and Torque of Selected Spring . . . . .	32
Figure 2.18	Selected Tension Springs . . . . .	33
Figure 2.19	CAV Unit Design . . . . .	34
Figure 2.20	Parts of CAV Unit . . . . .	35
Figure 2.21	Control Box for CAV Unit . . . . .	36
Figure 2.22	Final Version of Case of Control Box . . . . .	37
Figure 3.1	Simplified CAV Unit Geometry . . . . .	41
Figure 3.2	Geometrical Details of 3D CAV Unit Used for CFD Analyses . . . . .	41

Figure 3.3	Section View of 3D Geometry of Generated Mesh . . . . .	42
Figure 3.4	Close View of the Blade Part Mesh . . . . .	42
Figure 3.5	Analysis Results for Different Number of Elements for 160 mm CAV Unit for 600 m <sup>3</sup> /h . . . . .	43
Figure 3.6	Convergence Plot for 500 m <sup>3</sup> /h and 40 ° Blade Angle . . . . .	44
Figure 3.7	Velocity Streamlines at the Downstream for the Blade Angle 40° for 500 m <sup>3</sup> /h . . . . .	45
Figure 3.8	CFD Results for Moment and Blade Angle . . . . .	45
Figure 3.9	CFD Results for Pressure Drop and Blade Angle . . . . .	46
Figure 3.10	CFD Results for Pressure Drop and Air Flow Rate . . . . .	46
Figure 3.11	Pressure Distribution for Various Blade Angle with Flow Rate 500 m <sup>3</sup> /h . . . . .	47
Figure 3.12	Velocity Distribution for Various Blade Angle with Flow Rate 500 m <sup>3</sup> /h . . . . .	48
Figure 3.13	Eqn 2.2 and CFD Results Comparison for Pressure Drop Over CAV Unit . . . . .	48
Figure 3.14	Eqn 2.7 and CFD Results Comparison for Moment Over CAV Unit Blade . . . . .	49
Figure 3.15	Predicted Spring Moment and CFD Results . . . . .	50
Figure 4.1	Test Bench . . . . .	53
Figure 4.2	Schematic View of the Test Bench . . . . .	54
Figure 4.3	Close View of the Moment Measurement Setup . . . . .	55
Figure 4.4	CAV Unit Blade Angle Measurement . . . . .	56

Figure 4.5	Manometer and Flow Meter . . . . .	56
Figure 4.6	Dead Weight . . . . .	57
Figure 4.7	Load Cell Calibration . . . . .	58
Figure 4.8	Pressure Drop Measurement Setup . . . . .	60
Figure 4.9	Measurement of Bellows Pressure . . . . .	62
Figure 4.10	Close View of the Setup . . . . .	62
Figure 4.11	Measurement of Moment on the Blade Setup . . . . .	63
Figure 4.12	Details of Moment Measurement Setup . . . . .	64
Figure 4.13	Spring Constant Measurement Setup . . . . .	66
Figure 4.14	Air Velocity Measurement Setup . . . . .	67
Figure 4.15	Pressure Drop Values for Different Flow Rates and Blade Angles . . . . .	68
Figure 4.16	CAV Unit Pressure Drop and Bellows Inlet Pressure . . . . .	69
Figure 4.17	Torque on the CAV Unit Blade vs Blade Angle . . . . .	70
Figure 4.18	Spring Force values according to spring extensions . . . . .	71
Figure 4.19	Variations of Air Velocity at the Exit Plane of CAV Unit . . . . .	72
Figure 4.20	Ø160 mm CAV Unit Performance Result for 543 m <sup>3</sup> /h . . . . .	74
Figure 5.1	Pressure Comparison Between Experiment Results and CFD Results . . . . .	75
Figure 5.2	Moment Comparison Between Experimental Results, CFD Results and Spring Moment . . . . .	76
Figure 5.3	Pressure Drop Comparison Between Experimental Results, CFD Results and Theoretical Results . . . . .	77
Figure 5.4	Plexiglass CAV Unit . . . . .	78

Figure A.1 Ø160 mm CAV Unit Performance Result for 324 m <sup>3</sup> /h . . . . .	85
Figure A.2 Ø160 mm CAV Unit Performance Result for 354 m <sup>3</sup> /h . . . . .	85
Figure A.3 Ø160 mm CAV Unit Performance Result for 387 m <sup>3</sup> /h . . . . .	86
Figure A.4 Ø160 mm CAV Unit Performance Result for 444 m <sup>3</sup> /h . . . . .	86
Figure A.5 Ø160 mm CAV Unit Performance Result for 543 m <sup>3</sup> /h . . . . .	87
Figure B.1 Final Version of Circular CAV Unit . . . . .	89

## LIST OF ABBREVIATIONS

AHU	Air Handling Unit
ASHRAE	American Society of Heating, Refrigerating and Air-Conditioning Engineers
CAD	Computer Aided Drawing
CAV	Constant Air Volume
CFD	Computational Fluid Dynamics
HVAC	Heating Ventilating and Air Conditioning
SAD	Supply Air Duct
RAD	Return Air Duct
VAV	Variable Air Volume

## CHAPTER 1

### INTRODUCTION

Heating, Ventilating, and Air Conditioning (HVAC) systems are undeniably significant to create comfortable living zones for human beings. Indoor environments are always subject to the danger of fresh air deficiency if proper ventilation is not installed. Ventilation is necessary in buildings to supply fresh air, reduce odors, dust, bacteria, smoke and other contaminants that are harmful to human health.

Constant air volume unit (CAV) is a kind of flow controller which is used in supply and/or return ducts of HVAC systems. A CAV unit is a self-powered air flow rate regulator. Designed CAV unit resembles a butterfly valve which is used in water piping systems and it is explained in detail in Chapter 2. However, commercially available CAV unit has generally different shape as seen in Figure 1.1. Both have two main components namely control box and blade. Control box determines the blade position against aerodynamic torque by tension spring mechanism. Incoming air flow creates closing torque on the blade and tension spring creates opening torque. Balance of these two, keeps flow rate constant at preset value. Air flow rate can be adjusted by introducing pretension to tension spring of CAV unit. This can be done either manually or automatically. There is no difference between self-powered and motorized CAV unit in terms of air flow rate accuracy. However, self-powered CAV units have their own advantages. There is no need for electricity, which can be named as the major advantage.

The design and performance evaluation of the CAV unit is the basis of this work. At the design phase, benchmark tests are performed for typical CAV unit and com-

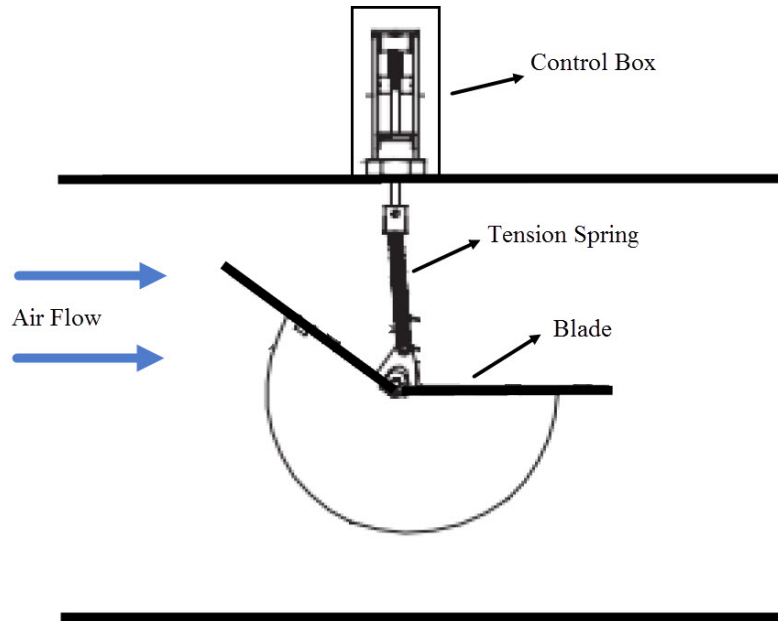


Figure 1.1: Typical CAV Unit

ponents are explained. After benchmark stage is over, CAV unit design is started. Since designed CAV unit closely resembles a butterfly valve, hand calculations are performed according to a two dimensional model which is taken from literature [1]. The model is used to calculate pressure drop and moment on the blade for known blade angles and air flow rate. After preliminary design stage is completed, CFD analyses are performed in order to eliminate probable errors and reduce prototype numbers. Additionally, CFD analysis results are used in experimental setup design. For example, pressure transducer range is decided according to CFD results. After design phase is completed, different kinds of laboratory experiments are performed on the designed CAV unit. Laboratory experiments are performed by using special test setups that are designed within this study. Then, the experimental results are used to validate numerical experiments. Finally, prototypes are tested in order to see whether the designed CAV units meet the requirements or not. The requirements that CAV unit should meet is given in Chapter 2.



## **1.1 General Information on HVAC Systems**

Heating, Ventilating and Air Conditioning (HVAC) systems can be divided into three categories, namely, all water systems, air-water systems, and all air systems.

### **1.1.1 All Water Systems**

Water is used as the working fluid in all water systems. Chilled water is used for cooling and hot water is circulated for space heating. Since HVAC plant (heating/cooling coil, water pump) supplies only water to the space, fresh air has to be supplied from another unit [2].

### **1.1.2 Air - Water Systems**

Air - water systems condition spaces by distributing both chilled water and hot water and conditioned air from a central system to individual spaces. Since specific heat and density of water is higher than air, cross sectional area of piping is smaller than that the ductwork to supply same cooling or heating capacity. However, controls are more complicated than all - air systems. Large office buildings, hotels are good application areas [2].

### **1.1.3 All Air Systems**

In all air system, air is used as working fluid and it is processed in AHU (Air Handling Unit). AHU mainly consists of dampers, mixing chambers, filters, cooling and heating coils, humidifiers, fans and blowers. Conditioned air is delivered to the space via air distribution system. Air distribution system includes ducts, dampers and diffusers. The duct that supplies the air to spaces is called Supply Air Duct (SAD) and the duct that returns the air from spaces is called Return Air Duct (RAD) [3]. Typical all air system can be seen in Figure 1.2. All air systems generally classified into

three categories namely dual-duct system, variable air volume system and single zone system.

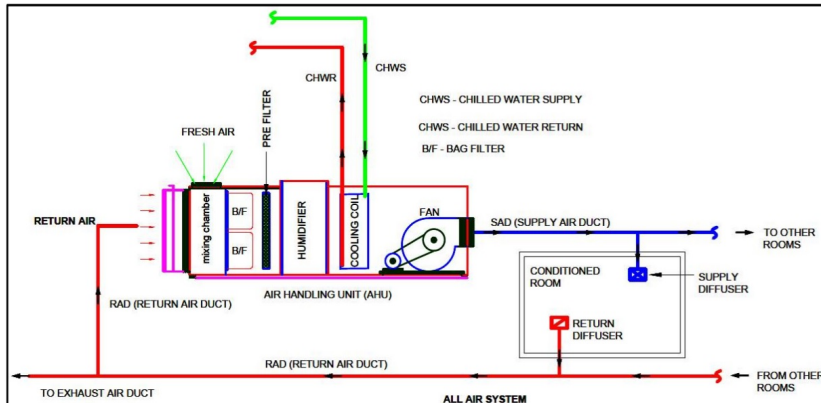


Figure 1.2: Schematic of All Air HVAC System [3]

### 1.1.3.1 Dual-Duct System

Central air handling unit distributes air to spaces via two parallel ducts. One carries cold air and the other one carries hot air so both heating and cooling air are provided at all times. To meet thermal load of the space, hot air and cold air is mixed by mixing damper which is controlled by room thermostat. Good control of humidity and temperature, ability to meet different zone loads are the main advantages. However, high energy consumption and huge space requirement are two main drawbacks [2].

### 1.1.3.2 Variable Air Volume Systems (VAV)

Variable air volume system which is shown in Figure 1.3 is a kind of ventilation system that is responsible for heating, ventilating, and air conditioning of the interior space. VAV systems are mainly controlled by a VAV box (or VAV valve) which can be seen in Figure 1.3. VAV system uses outside air mixed with return air at a central air handling unit. The air is then heated or cooled depending on the needs of the space. In simple VAV systems, temperature remains constant. Therefore, air flow rate must vary to compensate the temperature change. The system is typically very economical especially on a large scale [4].

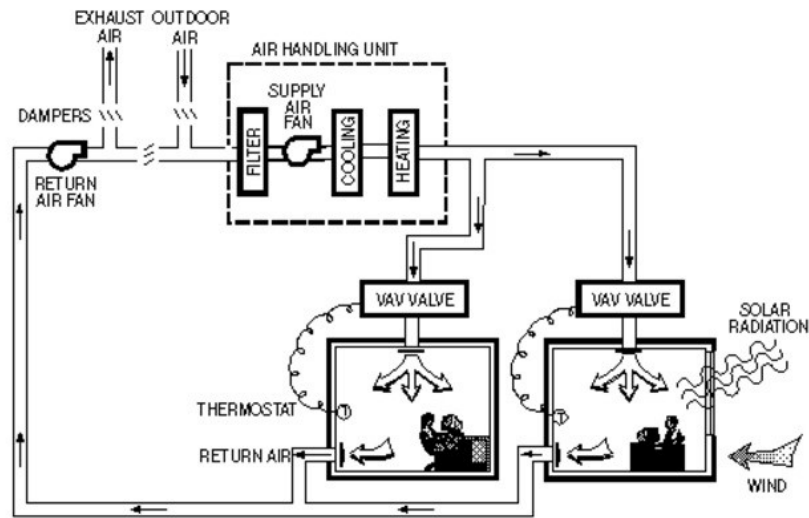


Figure 1.3: VAV System

VAV systems allow using smaller size fan when compared to full capacity running fan in constant air volume systems. Therefore, VAV systems decrease energy consumption and save energy so, high initial cost can be compensated in long term operations. Even though VAV systems have many advantages, there are some disadvantages. First and most important drawback of the VAV systems is high initial cost. Duct installation, dampers, VAV boxes, connecting VAV boxes to building automation system increase initial costs. VAV systems are more complex than CAV systems. VAV systems are commonly used for individual temperature control required applications. Large office buildings, residential apartments, conference rooms can be shown as some example application areas of VAV systems. Figure 1.4 shows a typical commercial VAV box.

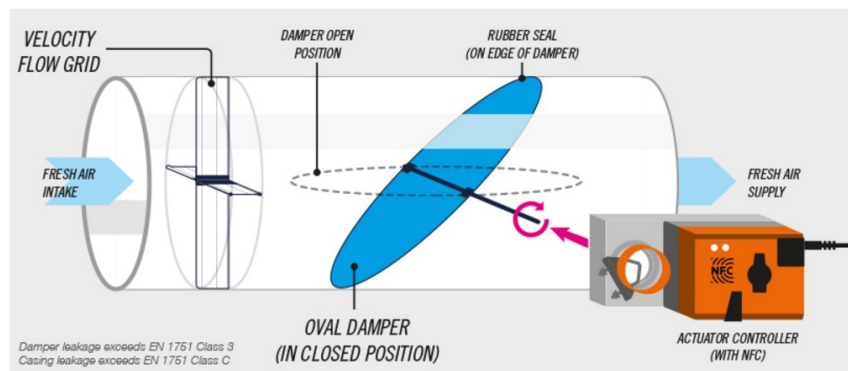


Figure 1.4: VAV Box [5]

### 1.1.3.3 Single - Zone System

This type of system supplies constant air volume. Constant air volume (CAV) systems are simple solution to HVAC needs of buildings. Because of its simplicity, CAV systems are very common. Constant air volume systems supply constant air volume into a building. All zones in the building receive same amount of air flow. Temperature control of incoming air flow can be done by using reheat coils in the air duct before the room entrance but this increases overall energy consumption. In Figure 1.5 single duct CAV system is shown. "SA" stands for supply air and "RA" means return air. CAV unit is positioned just before room entrance.

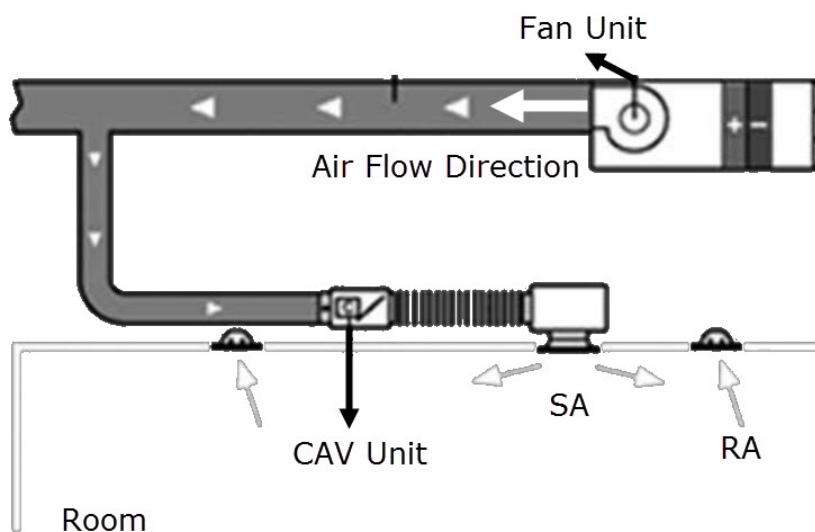


Figure 1.5: CAV System and CAV Unit [6]

CAV systems are mostly used in large areas that require same amount of ventilation. Single space buildings with little variance are the best application for CAV single duct systems. Warehouses are good example for CAV systems. There is one large volume and there is one heat load to meet. Low initial cost is the most crucial advantage in CAV systems. Design and construction is also easy. In Figure 1.6 typical CAV unit which is used in CAV systems is shown.



Figure 1.6: Mechanical CAV Unit

## 1.2 General Information on Typical Fan System and Operating Principle of CAV Unit

The total pressure rise that the fan must produce to move air is determined from the duct system characteristics. Therefore, it is necessary to consider the fan with its duct system. System curve can be expressed by Equation 1.1 .

$$\Delta p = RQ^2 \quad (1.1)$$

where R is the resistance coefficient and Q is the air flow rate. By using a calculated pressure drop at any particular flow rate, the value of R may be determined. The system characteristic can be plotted together with fan characteristic on the same graph as shown in Figure 1.7. It is seen from the figure the losses increase with the flow rate, since the right hand side term of Equation 1.1. represents the loss [7]. The intersection of the system characteristics and fan characteristics is the operating point. This means that the fan would deliver Q amount of air, if it operates with the characteristic shown in the Figure 1.7.

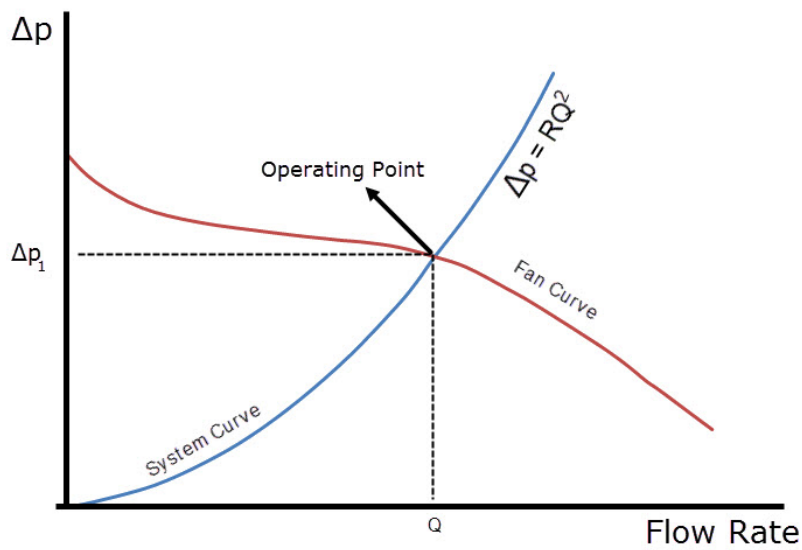


Figure 1.7: System Curve, Fan Curve and Operating Point [7]

### 1.2.1 Controlling Volumetric Flow Rate of a Fan

Fan discharge flow rate can be controlled by two different methods. The first method is changing the fan speed. Fan speed and flow rate are proportional. Therefore, when the fan speed is changed by variable frequency drive, flow rate changes accordingly.

Using flow control damper is another way to control flow rate. The outlet dampers on the system affects the system curve by their throttling action which means increase or decrease in the resistance coefficient in Equation 1.1. Increase in resistance causes the system curve to move towards left on the fan curve as seen in Figure 1.8. Constant air volume (CAV) device may be used as a flow control damper.

CAV units can be used in constant air volume systems in order to control volumetric flow rate in supply air duct and/or extract air duct. It reacts almost immediately to any pressure changes, so that the set volume flow rate is accurately controlled throughout the wide range of differential pressure.

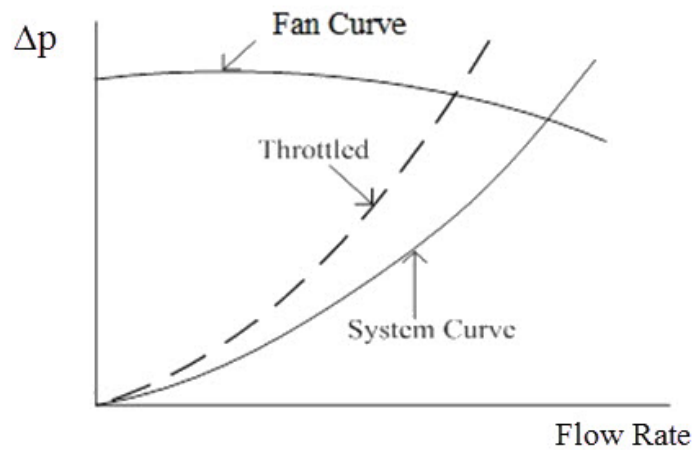


Figure 1.8: Change in System Curve with Throttling [8]

### 1.2.2 Operating Principle of CAV Unit

This design is taken from literature and used to explain operating principle of any CAV unit. Venturi air valve as seen in Figure 1.9. can be designed to supply constant air flow rate irrespective of change in the pressure differential over the unit. When pressure changes in the system, the cone moves to change air flow path in order to compensate pressure change, and this motion change air flow area which intends to keep airflow rate constant [9].

In Figure 1.10. operating principle of venturi type CAV unit is explained. When the static pressure is low, there is more space for air to pass through throat of the valve. When pressure is high, pressure on the upstream side pushes the cone and restricts the air flow rate. Therefore, flow rate can be kept constant. When the static pressure decreases cone moves back and increases the air flow area to keep air flow rate constant.

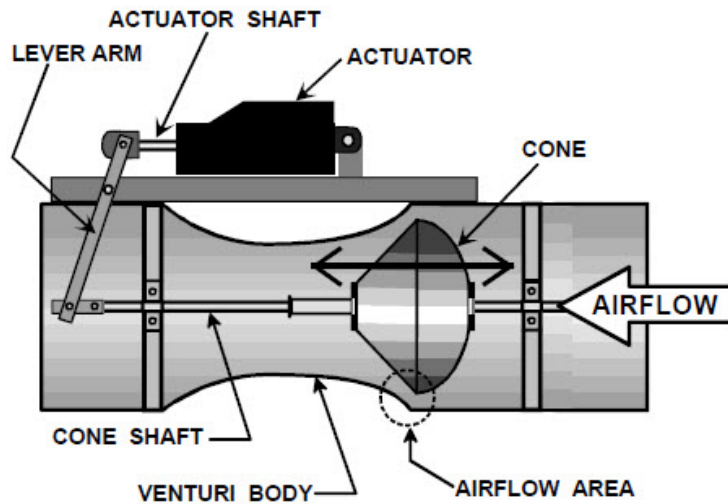


Figure 1.9: Venturi Shape CAV Unit [9]

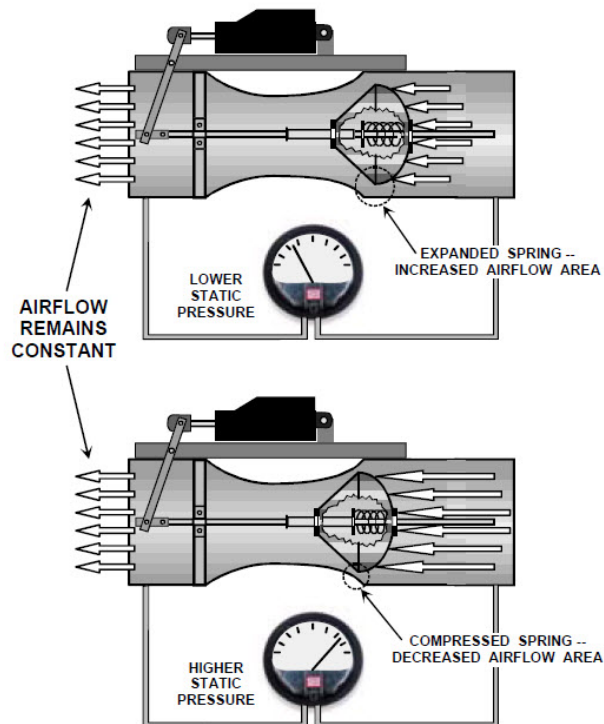


Figure 1.10: Operating Principle of a Venturi Type CAV Unit [9]

### 1.3 Literature Survey

In literature, there are patents related with CAV unit. Even though they are quite old, operating principles are still applicable. There are also many studies on butterfly



valves in literature. Since designed CAV unit is a butterfly valve for air ducts, these studies will be reviewed.

Nishizu, Okubo and Wada [10] invented an automatic CAV unit and they patented in 1974. This unit has a different type of valve which gradually decreases and increases air passage to minimize vortices and noise that is emitted from the unit. This also gives the unit stability while operating. Their CAV unit is designed for rectangular ducts and it has an electric motor to adjust pretension of spring. Pretension of spring determines the air flow rate which will be kept constant.

Finkelstein, Baumeister and Haaz [11] in 1979 patented their invention, which was a regulator valve for maintaining air flow rate constant. This CAV unit is designed for circular ducts. CAV unit blade is like butterfly valve and a bellows is attached to eliminate excessive oscillation on the valve. Set value of air flow rate is adjusted by means of a servomotor thereby remote control is possible. Servomotor changes pretension of tension spring. Higher pretension means higher air flow rate.

Leutwyler et al. [12] studied numerically for the flow of a compressible flow through butterfly valve. He tried to predict aerodynamic torque on the valve by using Fluent. Calculated data was compared with experimental results. Different grid sizes and turbulence models were also used. Among Spalart - Allmaras,  $k-\omega$ ,  $k-\epsilon$  turbulence models  $k-\epsilon$  model was chosen because of moderate computational time and agreement with experimental data.

Morris et al. [13] investigate butterfly valve performance experimentally. In the study, air was used as a working fluid. Investigation is mainly about elbow position at the downstream side. Aerodynamic torques on the valve, pressure drops, mass flow rates were measured. They concluded that when butterfly valve positioned at eight diameters to elbow, effect of the elbow is small.

Studies which are reviewed below made for butterfly valves which operate in water environment. These studies have good examples for CFD analysis and experiments so they have valuable information.

Henderson et al. [14] studied numerically a butterfly valve which was used in hydroelectric power plant. In order to predict variation of the hydrodynamic torque according to blade angles ANSYS CFX software was used and modeling was done in quasi-steady manner. In other words, for different blade angle, hydrodynamic torque calculated in steady state.  $k - \omega$  Shear Stress Transport (SST) was used for turbulent closure. Henderson concluded that for valve angles greater than  $20^\circ$ , flow behind the valve was dominated by unsteady vortices. Moreover,  $20^\circ$  and  $30^\circ$  blade angle states were solved in unsteady to obtain good convergence of residuals. Obtained results were compared with field measurement. Even though both data have the same trend, they differ from each other up to 25%.

Sarpkaya [15] studied experimentally on torque and cavitation characteristics of butterfly valve. Then, Sarpkaya managed to determine hydrodynamic torque, flow coefficients and cavitation for butterfly valves using semi empirical equations.

Kimura et al. [16] tried to determine pressure loss characteristics and cavitation stages for a butterfly valve. Pressure loss characteristics were found by experiments. First, frictional loss on the system (without butterfly valve) was measured. Then, Kimura calculated net pressure loss of the butterfly valve by subtracting the frictional loss from valve pressure loss. Kimura concluded that at fully open blade position pressure loss increases in the order of flat blade, round hub type blade and square hub type blade. He also concluded that for middle valve openings pressure loss does not depend on the valve shape since flow fluctuations at the downstream become larger.

Sandalcı et al. [17] tested two different sizes butterfly valves. Tests were performed at three different water flow rates and five different blade angles. Test results were used to determine loss and flow coefficient of the valves. They proposed correlations to predict performance coefficients for different sizes of butterfly valves.

## 1.4 Objectives and Outline of the Thesis

The aim of this study is to design a constant air volume unit to maintain air flow rate constant for HVAC systems. Mathematical model of CAV unit is developed. This model is capable of relating aerodynamic torque and spring constant. Moreover, pressure drop can also be predicted by using this model. CAV unit is also modeled numerically by using Fluent 16.0. Pressure drop, aerodynamic torque on the blade are monitored. Experimental studies are also performed for full scale CAV unit. Comparison between mathematical and numerical model is done. Furthermore, both model data are also compared with experiment results. Design process is given as in flow chart in Figure 1.11

In Chapter 2, a butterfly like CAV unit is modeled as two dimensional. Pressure drop over the CAV unit and moment on the blade is predicted according to various blade angles for constant air flow rate. A control mechanism is also proposed. Proposed control mechanism contains a tension spring and its spring constant is also predicted.

In Chapter 3, CFD analysis of CAV unit is presented. Obtained pressure drop values and moment values are compared that are found in Chapter 2.

In Chapter 4, experimental setup and experiment procedures for some measurements are given. Collected results are compared with CFD results. Moreover, performance evaluation tests are explained and results of the tests are given.

In Chapter 5, results and gained experiences are shared.

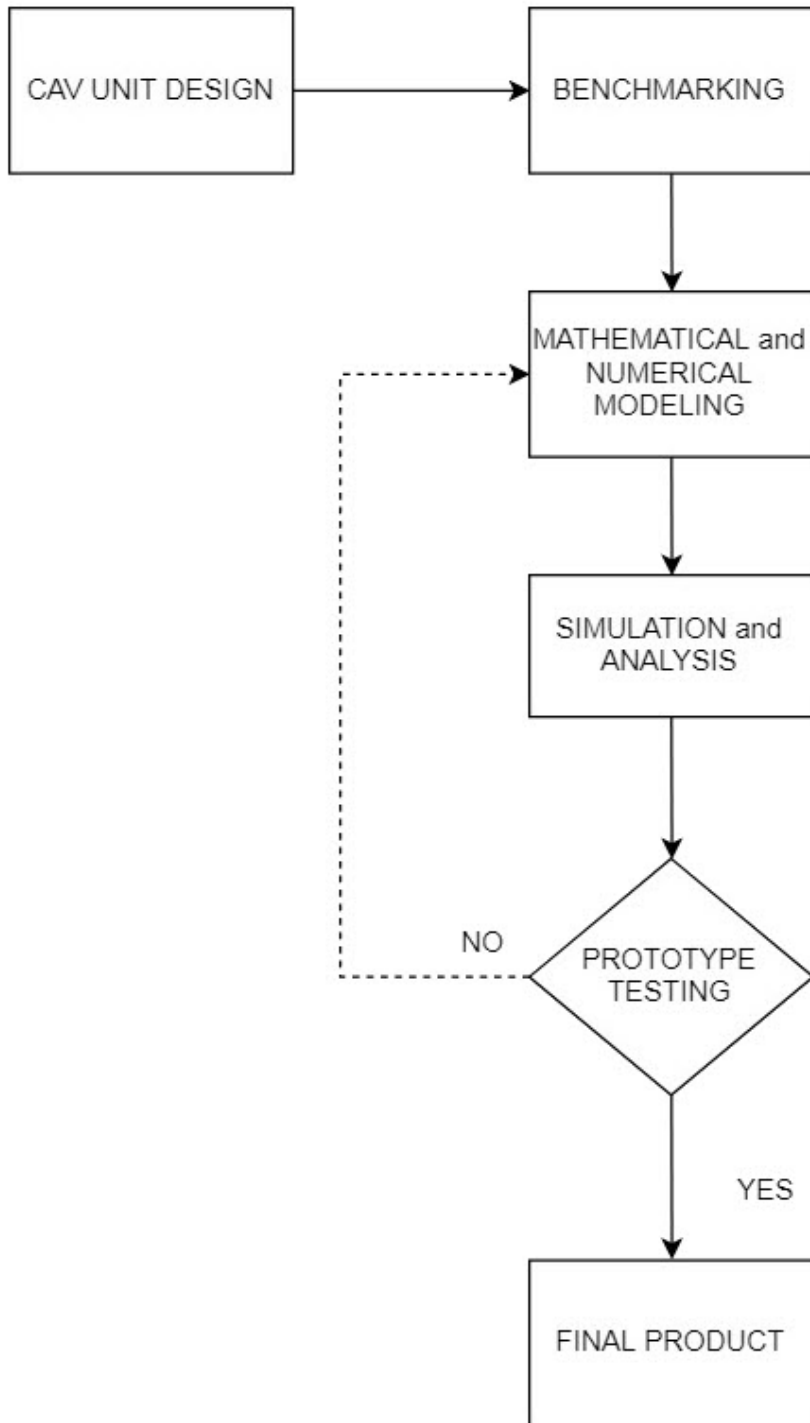


Figure 1.11: Flow Chart of CAV Unit Design

## CHAPTER 2

### DESIGN OF THE CONSTANT AIR VOLUME UNIT

#### 2.1 Design Goals, Limitations and Strategy

The constant air volume device (CAV unit) to be designed should supply constant air flow rate into HVAC zones even if system characteristics of the whole system is changed by some external effects like clogging of outlet grills or deactivating some parts of air duct by using shut-off damper. Since CAV unit is used in constant air volume systems, fan speed is kept constant which means that fan curve does not change. Therefore, changes on the system curve due to pressure change must be tolerated to keep air flow rate at constant value. Various pressure drop can be obtained from CAV unit so overall pressure value can be maintained constant. As seen in Figure 2.9. for a constant pressure value, constant air flow rate can be obtained from supply fan.

Designed CAV unit closely resembles a butterfly valve. Two dimensional model of butterfly valve is considered to obtain pressure and moment values. Flow in downstream of the valve is highly turbulent especially for high blade angles. Therefore, there is no general moment equation that gives moment values exactly. To predict moment on the blade of CAV unit a model is used and details of the model is given later in this chapter.

Design limitations of CAV unit can be listed as follows:

- Air flow rate should be kept constant from 50 Pa to 1000 Pa differential pressure

between inlet plane of the CAV unit and exit plane of the CAV unit.

- Air flow rate sensitivity should be in the range of  $\pm 10\%$  of set flow rate.
- CAV unit should be able to operate inlet air velocity between 2-10 m/s.
- There should be no electrical component, the CAV unit should be mountable in any orientation and it should be easily manufactured.

Design is started with benchmark tests. Two commercially available CAV units are tested to see whether these devices can supply constant air flow rate or not. These benchmark tests are performed at research and development laboratory of the factory. Test setup details and test procedures are explained in later sections. One of the CAV unit is able to maintain air flow rate constant according to increasing pressure drop. Therefore, this CAV unit is taken for further investigations. Taken CAV unit is disassembled and each parts of it are examined. Benchmark tests and examination of the unit give new ideas about how constant air volume device can be designed and manufactured.

## **2.2 Examination of a CAV Unit, Benchmark Tests and Results**

In this section a commercially available CAV unit which is shown in Figure 2.1 is examined. First, components of the unit is explained. Second, two CAV units which have same geometrical features are tested to check whether constant air flow rate can be supplied from the devices or not. Note that two CAV units are manufactured from different manufacturer.

## 2.2.1 Commercial CAV Unit and Components

Commercial CAV unit which is shown in Figure 2.1. has an asymmetric blade and it tends to close when it is exposed to air flow. It uses tension spring to control blade position. For higher blade angle, tension spring generates higher force which creates higher torque on the blade. Air flow rate can be adjusted by increasing pretension of the spring using flow rate setting mechanism. The unit also uses piston to eliminate excessive oscillations of blade.

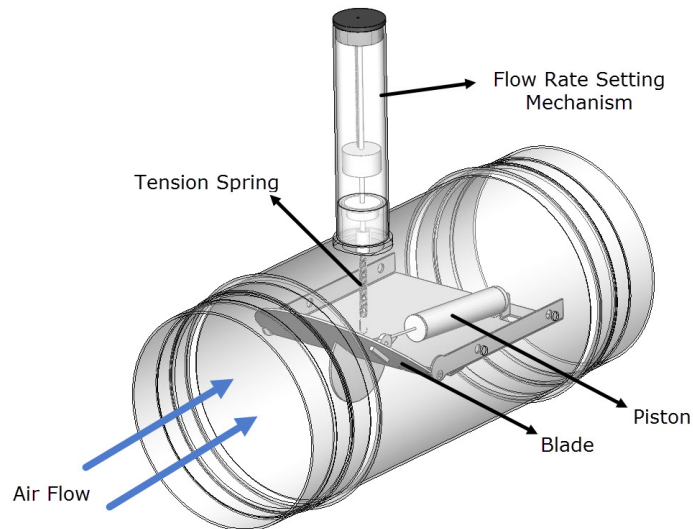


Figure 2.1: Commercially Available CAV Unit

### 2.2.1.1 Blade of CAV Unit

CAV unit blade has an asymmetric blade shape which is shown in Figure 2.2. Upper portion of the blade has circular cross section and lower portion of the blade has an elliptic shape. Due to this configuration, air flow creates closing torque on the blade.

This design utilizes piston like damper to eliminate blade oscillation. Piston is tightly assembled to prevent uncontrolled air leakage from inside of the piston body. One end of the piston is mounted to upper blade and the other end of the piston is mounted to chassis. Figure 2.3 shows piston assembly in CAV unit.

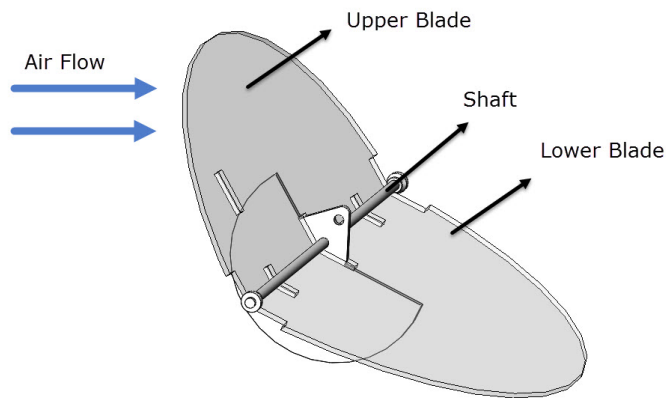


Figure 2.2: CAV Unit Blade

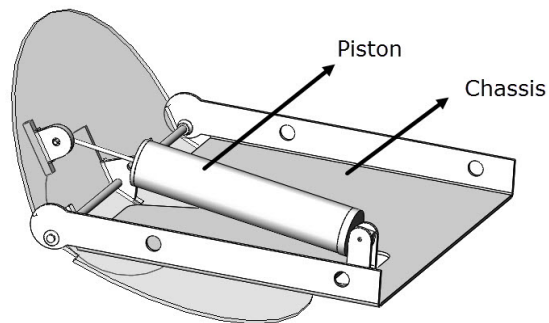


Figure 2.3: Assembly of Piston

### 2.2.1.2 Control Box of CAV Unit

Control mechanism is located on top of the CAV unit as seen in Figure 2.4. Pretension of the spring can be increased by screw. When screw is rotated, tension spring holder moves up or down. This movement adjusts the pretension of spring. Higher pretension gives higher air flow rate.



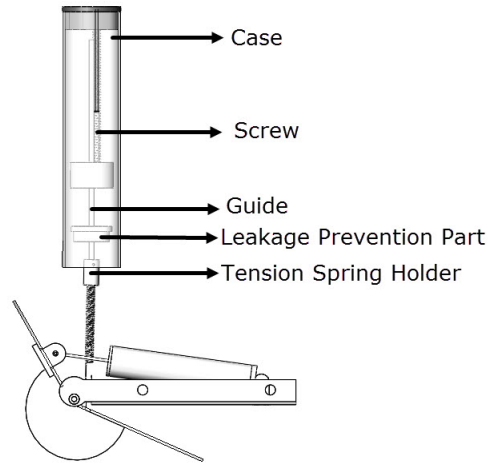


Figure 2.4: Control Box for CAV Unit

### 2.2.2 Benchmark Tests and Results

Two commercially available 200 mm diameter CAV units are tested. Both have same blade geometry. Flow rate control mechanisms are the same for two devices. However, their spring stiffness are different. Product A has stiffer tension spring than Product B. Since both are claimed that the CAV unit operates for the same air flow rate, it is expected that their spring stiffness should be close to each other.

Product A and Product B are separately mounted to the test setup which is explained in Chapter 4. Both of them are tested for the same preset flow rate values which is  $500 \text{ m}^3/h$ . Additionally, Product A is tested for  $800 \text{ m}^3/h$  air flow rate and Product B is tested for  $700 \text{ m}^3/h$  air flow rate. By increasing differential pressure over the CAV unit, air flow rate is measured and recorded. Obtained data for product A are presented in Figure 2.5 and in Figure 2.6. Straight lines in figures represent  $\pm 10\%$  allowable deviation from set air flow rate.

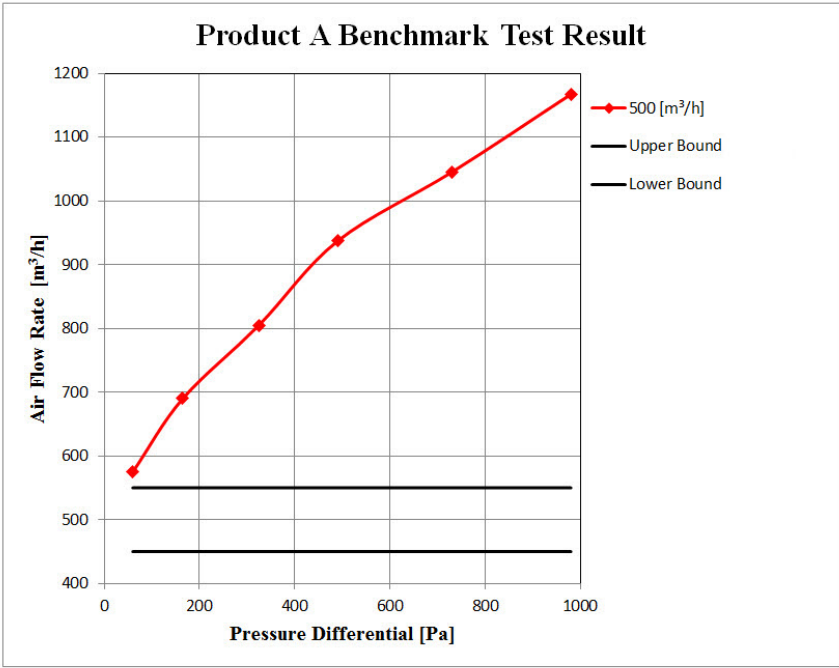


Figure 2.5: Benchmark Test Results for 200 mm Diameter CAV Unit for 500m<sup>3</sup>/h

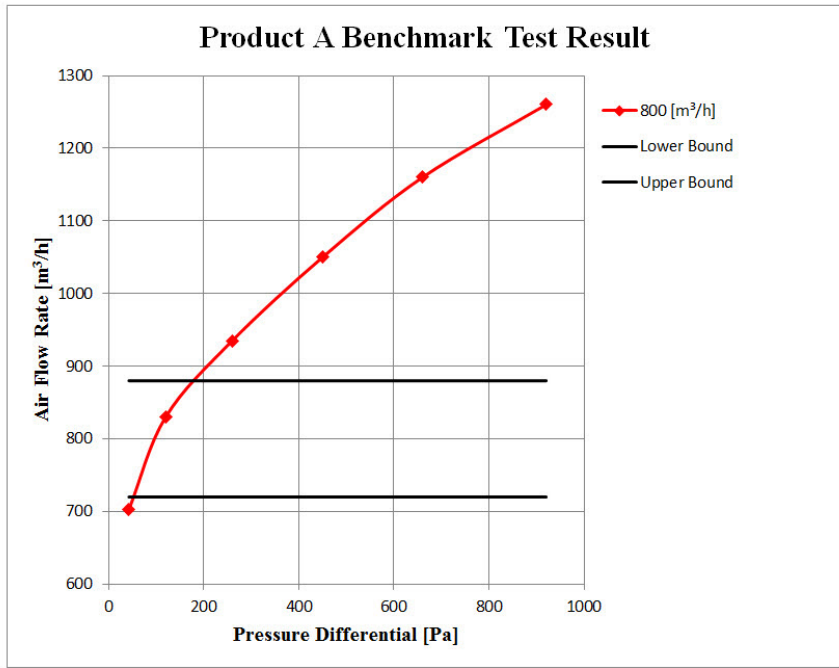


Figure 2.6: Benchmark Test Results for 200 mm Diameter CAV Unit for 800m<sup>3</sup>/h

Obtained data for product B are presented in Figure 2.7 in Figure 2.8. Straight lines in figures represent  $\pm 10\%$  allowable deviation from set air flow rate.

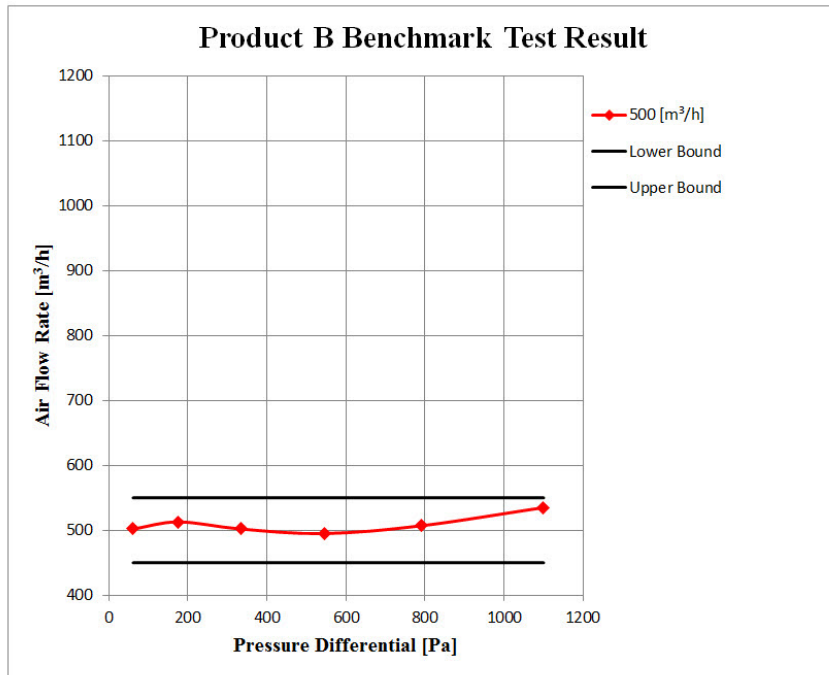


Figure 2.7: Benchmark Test Results for 200 mm Diameter CAV Unit for  $500\text{m}^3/\text{h}$

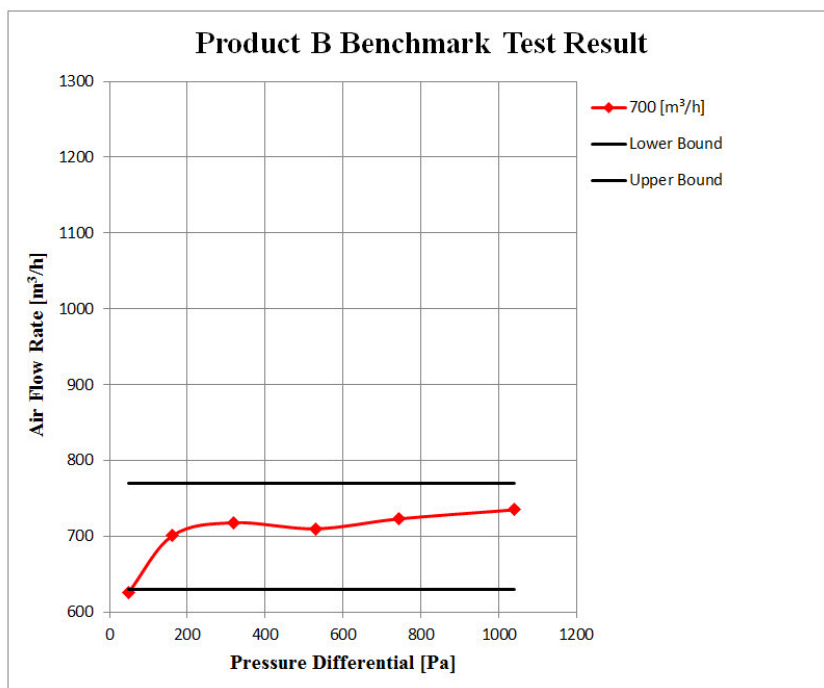


Figure 2.8: Benchmark Test Results for 200 mm Diameter CAV Unit for  $700\text{m}^3/\text{h}$

As seen in Figure 2.5 and in Figure 2.6 Product A does not operate properly. It can not maintain set flow rate against increasing differential pressure. However, Product

B gives acceptable results as seen in Figure 2.7 and in Figure 2.8. Even though air flow rate fluctuates, it lies in the allowable limits.

Results that are obtained after benchmark tests as follows:

- Spring is the crucial element of the CAV unit and its spring stiffness should be determined carefully. Blade position is controlled by the tension spring. When the system pressure increases, blade of CAV unit should move to opening direction to restore initial system pressure or when the system pressure decreases, blade of CAV unit should move to closing direction to restore initial system pressure.
- Higher flow rates can be obtained by increasing pretension of the spring.
- In order to eliminate excessive oscillation a damper like mechanism is needed.

After performing some benchmark tests and understanding the mechanism of air flow throttling, air flow throttling device or in other words CAV unit is designed in following sections. Spring stiffness is predicted by mathematical model.

### 2.3 Design of CAV Unit

Since CAV unit to be designed is a kind of butterfly valve, general shape of the unit is somewhat known. Moreover, in the market air ducts are produced in certain sizes. Therefore, diameter of CAV unit must be suitable for the air ducts in the market for easy mount. Ø160 mm diameter CAV unit is modeled and design procedure is explained in the following sections.

In Table 2.1. air flow rate ranges for various inlet air velocities are given. Designed CAV unit operates between  $145m^3/h$  and  $724m^3/h$ . Moreover, Reynolds number is also given. According to these Reynolds number values the flow is turbulent since all the Re numbers above critical Re Number of 2300 [18].

$$Re_D = \frac{\rho V D}{\mu} \quad (2.1)$$

Table 2.1: Air Flow Rate Ranges and Re Numbers for Ø160 mm CAV Unit

CAV Unit Diameter Ø160 mm		
Air Velocity [m/s]	Air Flow Rate [ $m^3/h$ ]	Re Number
2	145	20888
3	217	31333
4	290	41777
5	362	52221
6	434	62665
7	507	73109
8	579	83554
9	651	93998
10	724	104442

### 2.3.1 Operating Characteristics of CAV Unit

In Figure 2.10. schematic of CAV unit is given. CAV unit keeps set air flow rate constant over the entire differential pressure range. Incoming air flow through partially open CAV unit blade, creates both drag force and lift force on the blade. Center of rotation of the blade and the resultant force of drag and lift forces do not coincide and this generates closing torque over the blade. Closing torque changes according to blade angle and air flow rate. Moreover, pressure drop over CAV unit blade also depends on blade angle and air flow rate. If there is a change in static pressure of the system, by arranging CAV unit blade position air flow rate can be kept constant.

In Figure 2.9. typical fan curve and system resistance curve is shown.

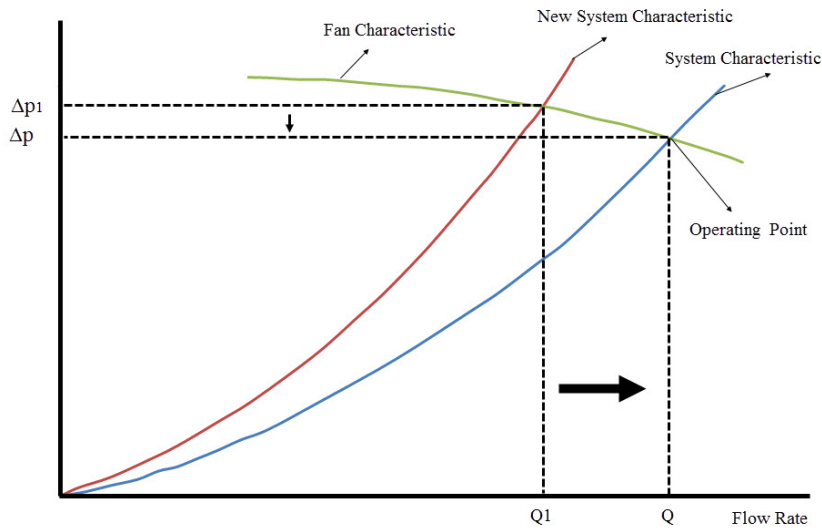


Figure 2.9: Typical fan curve and system resistance curve

CAV unit affects the system curve by increasing or decreasing the resistance to flow through its throttling action. This changes on the system characteristic curve is shown by Figure 2.9 . Green line shows typical fan curve and it is labeled as “Fan Characteristic”. The blue line shows the system curve and it is labeled as “System Characteristic”. The intersection of these two curves is called “Operating Point”. To be able to obtain air flow rate "Q",  $\Delta p$  amount of pressure differential is required from the fan. Without external influences, the fan operates only at this point. However, some disturbances might be introduced to the system. These disturbances create new

system characteristic which is labeled as "New System Characteristic" on the red line and changes the operating point of the fan. Therefore,  $\Delta p_1$  amount of pressure rise is required to overcome new system losses to supply "Q1" amount of air flow rate. Since the objective is to keep air flow rate constant at initial flow rate "Q", external disturbances must be compensated by CAV unit. As CAV unit blade changes its position, it can create different system curves. As an example, when external disturbances increase resistance on the system, CAV unit opens air flow passage to decrease resistance. Figure 2.9. explains that what happens to the system characteristic while CAV unit is operating. Figure 2.10. shows how CAV unit throttles air flow rate.

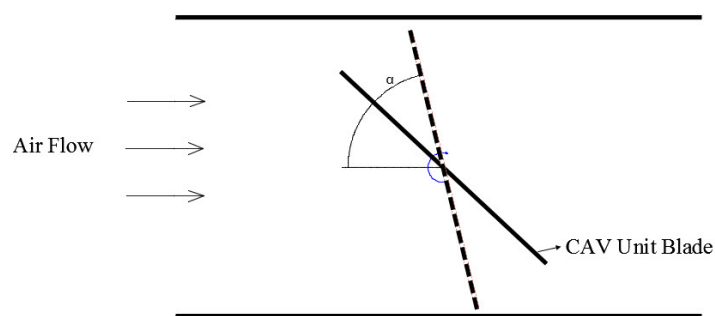


Figure 2.10: Schematics of CAV Unit

Dash lines in the Figure 2.10 shows the initial position of CAV unit blade. If the resistance on the system increases, air flow rate decreases. To keep air flow rate constant, resistance on the system should be decreased. Moving CAV unit blade in counter clockwise direction supplies more opening for air flow, this decreases the resistance on the system and restore the initial system characteristics. New blade position is shown by solid lines. As a result, flow rate is kept constant by changing the position of CAV unit blade.

### 2.3.2 Calculation of Pressure Drop and Moment on the CAV Unit Blade

In this section 2D modeling of CAV unit is presented. Schematic of CAV unit can be seen in Figure 2.11. It has a circular shape and attached to a shaft which passes through middle of the air duct. Wake region occurs behind the blade.

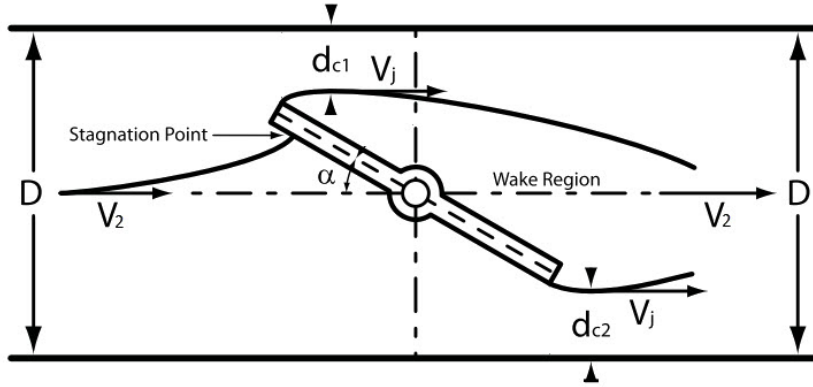


Figure 2.11: 2D Model of CAV Unit [1]

The Borda-Carnot equation which is Equation 2.2 is an empirical relation that describes pressure losses in a fluid undergoing an abrupt expansion in flow area. These losses are due to turbulence in the wake regions.

$$\Delta p = \xi \frac{1}{2} \rho (\Delta V)^2 \quad (2.2)$$

$\Delta p$  is pressure loss,  $\rho$  is the fluid density and  $\Delta V$  is the reduction in average velocity between vena contracta,  $V_j$ , and CAV unit outlet  $V_2$ .  $\xi$  is an empirical, dimensionless loss coefficient which can be taken as 1 for butterfly valves [1].  $D$  is CAV Unit diameter and the same for inlet and outlet.  $d_{c1}$  and  $d_{c2}$  are the widths of vena contracta.  $V_j$  is jet velocity and  $V$  is the average velocity. Since incoming air flow rate is known  $V_j$  can be calculated by using Equation 2.3.

$$Q = A.V \quad (2.3)$$

$Q$  is air flow rate,  $A$  is air flow area and  $V$  is air velocity. Change in the blade angle,



decreases or increases the air flow area.

$d_{c1}$  and  $d_{c2}$  can be calculated by using following equations assuming blade diameter is equal to CAV unit diameter.

$$d_{c1} = C_{c1} \frac{\eta}{2} (1 - \sin\alpha) \quad (2.4)$$

$$d_{c2} = C_{c2} \frac{\eta}{2} (1 - \sin\alpha) \quad (2.5)$$

where  $\alpha$  is blade angle,  $\eta$  is CAV Unit diameter,  $C_{c1}$  and  $C_{c2}$  are contraction coefficient for upper and lower jet.  $C_{c1}$  and  $C_{c2}$  are tabulated in Table 2.2 according to increasing blade angle [19].

Table 2.2: Contraction Coefficients

Blade Angle [°]	$C_{c1}$	$C_{c2}$
10	0.904	0.578
20	0.851	0.571
30	0.808	0.569
40	0.768	0.57
50	0.734	0.574
60	0.701	0.58
70	0.67	0.587
80	0.64	0.597
90	0.611	0.611

$V_j$  velocity can be calculated by using Equation 2.6. and in Figure 2.12.  $V_j$  values are given for increasing blade angle.

$$DV = (d_{c1} + d_{c2})V_j \quad (2.6)$$

By using Equation 2.3. air velocity which is  $V_j$  can be calculated for different blade

angle values. As an example, 160 mm diameter CAV unit for 500 m<sup>3</sup>/h is considered. In Figure 2.12 jet velocity variations according to blade angle is given. As seen in the figure, for high blade angles, very high flow rates can be obtained. Inlet and outlet velocity is equal since areas are the same.  $V_j$  is the same as outlet or inlet velocity for zero degree blade angle which means blade is fully open.

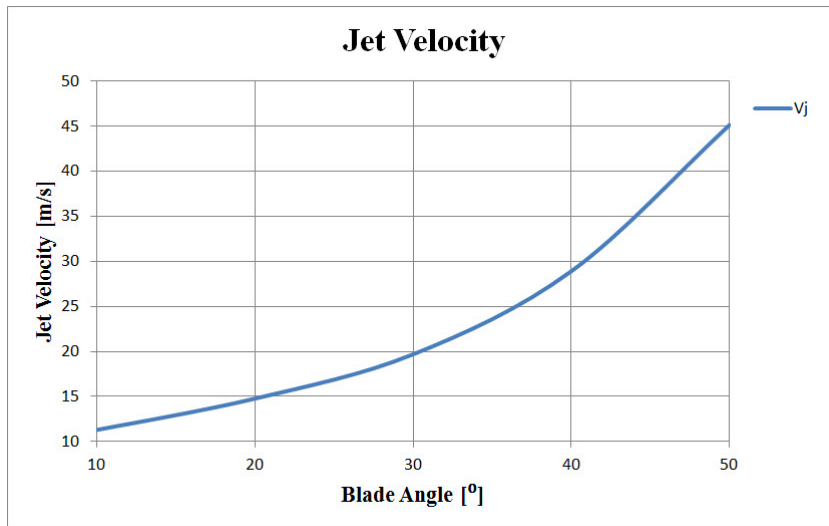


Figure 2.12: Jet Velocity According to Blade Angle

By using Equation 2.2. pressure drop for CAV unit blade can be calculated. Pressure drops according to blade angles is given in Figure 2.13 .

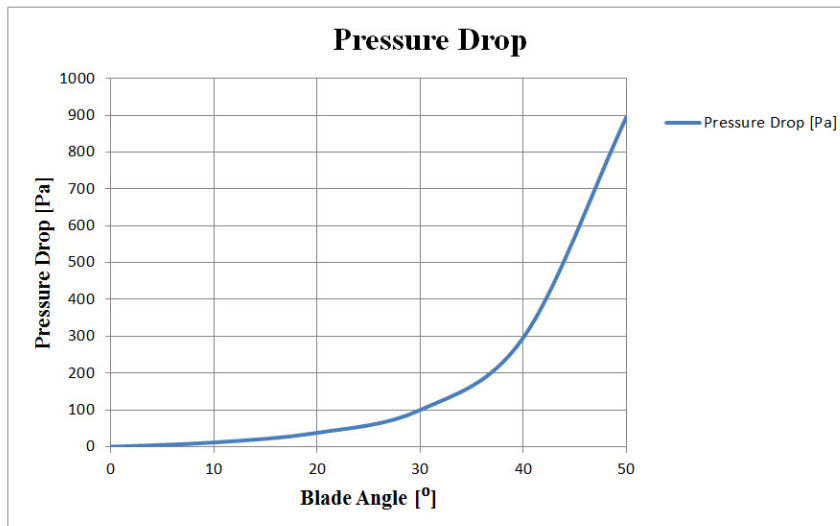


Figure 2.13: Calculated Pressure Drop According to Blade Angle

By knowing  $V_j$  values aerodynamic torque on the blade can be calculated by using

Equation 2.7 which is proposed by Sarpkaya [15].

$$T = \frac{3\pi}{8} \frac{\sin 2\alpha}{(4 + \sin \alpha)^2} \rho V_j^2 \eta^2 \delta \quad (2.7)$$

In Equation 2.7 T is aerodynamic torque about rotation axis of blade,  $\rho$  is density of air,  $\eta$  is CAV Unit diameter,  $\delta$  is blade diameter. Note that CAV unit diameter and blade diameter is assumed as the same. Calculated torque values are given in Figure 2.14.

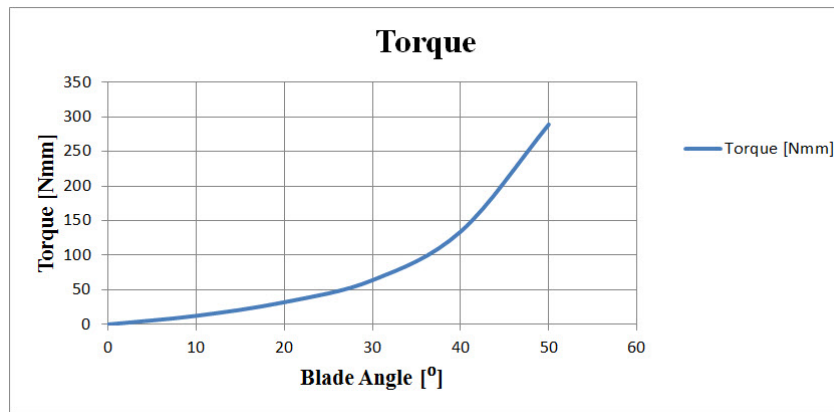


Figure 2.14: Calculated Torque According to Blade Angle

In order to keep air flow rate constant aerodynamic torque on the blade due to air flow must be balanced. For balancing mechanism a tension spring and suitable moment arm is proposed and they will explained in following section.

### 2.3.3 Mathematical Relations between Torque on The Blade and Extension of Tension Spring

When aerodynamic torque is known for various blade angles and air flow rate, torque balancing mechanism can be designed. In this study, as a balancing mechanism, tension spring and moment arm system is proposed. Balancing mechanism tries to increase air flow area whereas incoming air flow tries to decrease air flow area. Schematic of balancing system is given in Figure 2.15. The force,  $F$ , applied by the spring changes according to blade angle. High blade angle exposed to high aerodynamic torque for same air flow rate so high balancing force is needed. Tension spring is attached to a tire. It's radius acts as a moment arm. Tire is connected to blade rigidly via shaft. For high blade angle tension spring extends more and creates high force values. Therefore, keeping air flow rate for high blade angles is possible.

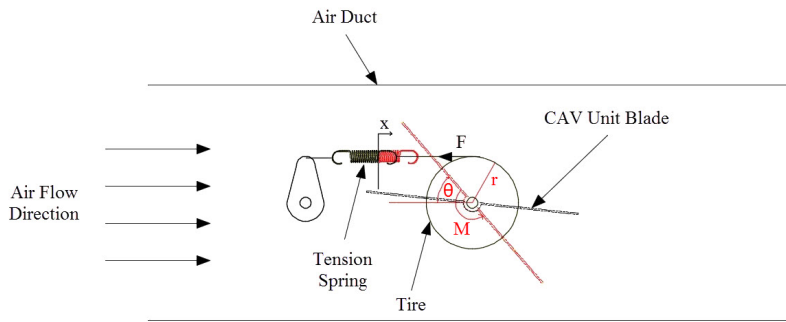


Figure 2.15: CAV Unit (unstretched and stretched spring position)

Moment created by spring force can be expressed by Equation 2.8.

$$\Sigma M = F.r \quad (2.8)$$

where  $F$  is spring force,  $\theta$  is blade angle,  $r$  is moment arm and  $M$  is torque on the blade due to spring force and moment arm. Spring force  $F$  can also be written as

$$F = k.x \quad (2.9)$$

where  $k$  is spring constant and  $x$  is the displacement of tension spring which is also proportion of circumference of the tire. Then, Equation 2.8 can be written as

$$\Sigma M = k.x.r \quad (2.10)$$

Then,

$$\Sigma M = k.2.\pi.r.\frac{\theta}{360}.r \quad (2.11)$$

simplify Equation 2.11

$$\Sigma M = k.\pi.\frac{\theta}{180}.r^2 \quad (2.12)$$

Equation 2.12 states that there is a linear relation between moment on the CAV unit blade and blade angle  $\theta$  when moment arm is kept constant and same spring is used. Therefore, tension spring - blade - tire combination can only give linear response to moment that created by aerodynamic forces on the damper blade.

In Equation 2.12 spring constant and tire radius are unknown. Tire radius is limited by geometrical constraints. Therefore, tire radius which is moment arm is selected as 20 mm. Then, calculated spring constant values can be drawn for different blade angles and it is given in Figure 2.16 .

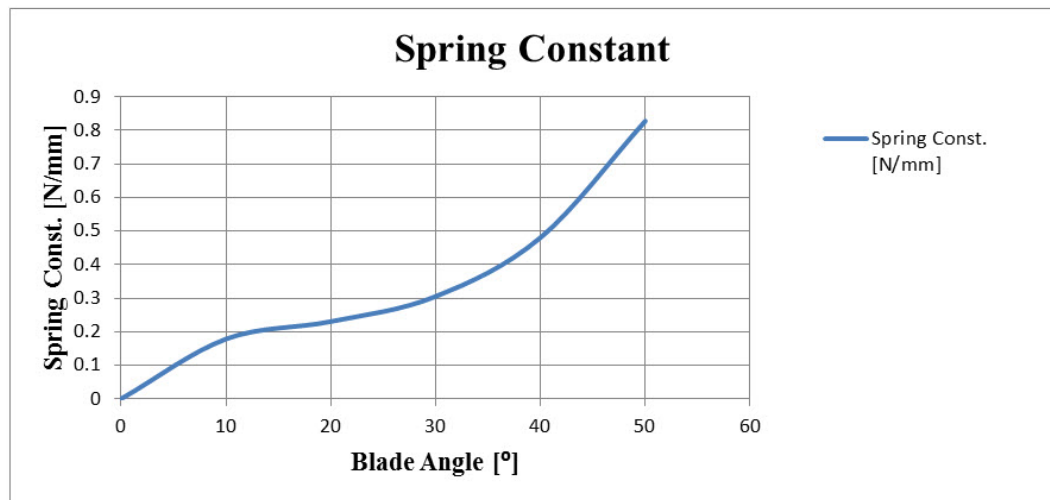


Figure 2.16: Calculated Spring Constant vs Blade Angle

Figure 2.16 shows that spring constant changes according to blade angle. This means that for every blade angle different spring should be used and it is not practical. However, in practice only one spring is used to balance aerodynamic torque on the blade. Therefore, average spring constant is used for following calculations.

The reason for obtaining various spring rates is that calculated torque values do not depend linearly on the blade angle. Aerodynamic torque values are calculated by using Equation 2.7. This is also called Kirchhoff-Rayleigh model. This model over predicts torque values for high blade angles.

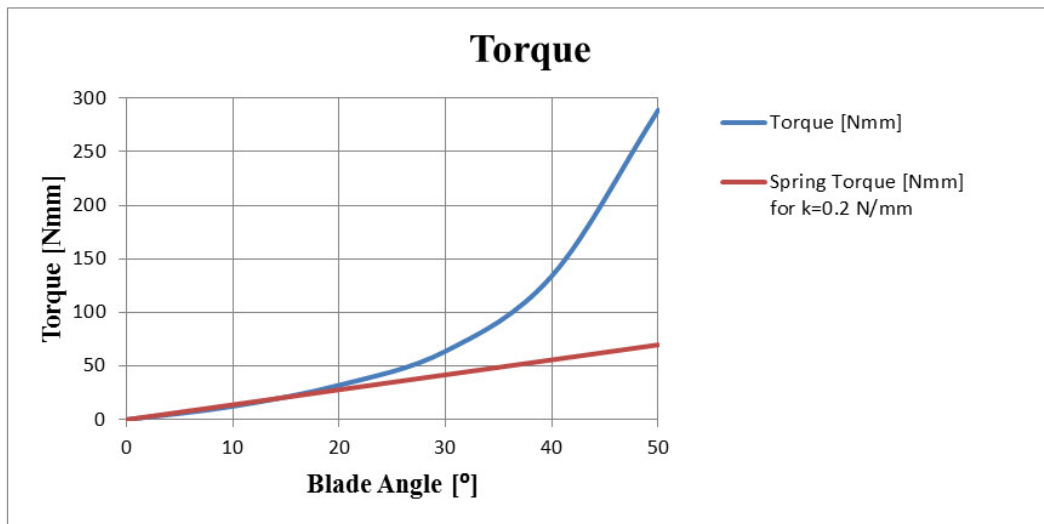


Figure 2.17: Comparison of Calculated Aerodynamic Torque and Torque of Selected Spring

Figure 2.17 compares Equation 2.12 when the spring constant is taken as 0.2 N/mm and tire radius is taken as 20 mm and the calculated aerodynamic torque by Equation 2.7 . It shows that up to 20° blade angle both torques are in agreement. However, for higher blade angles aerodynamic torque calculation model is not adequate.

### 2.3.4 Tension Spring Selection

Since flow rate throttling must be done without utilizing any electrical component in CAV unit, an actuator cannot be used to regulate blade position. Blade position control can be achieved by proper combination of tension spring and tire which is used as moment arm to adjust spring force. Moreover, use of tension spring makes mounting of CAV unit independent of air duct orientation. In other words, CAV unit can be mounted in horizontal or vertical direction. Therefore, tension spring is the main component in the constant air volume device. Spring is the component which determines the blade opening amount in other words it determines the pressure drop over the CAV unit. For example if opening area is larger than the “right” amount, air flow rate will be higher than the desired amount. Right spring selection also determines the flow rate sensitivity.

According to calculated average spring constant, and geometrical limitations some tension springs are selected and they can be seen in Figure 2.18. Spring constants of selected tension springs is measured and suitable ones are used in CAV unit. Both measurement details and performance tests are explained in later sections.



Figure 2.18: Selected Tension Springs

## 2.4 CAD Model of CAV Unit

According to 2D mathematical model of CAV unit, 3D solid model is drawn as seen in Figure 2.19. It uses bellows as a damper and tension spring for creating restoring torque on the blade and it also contains less parts when compared with other commercial products so this means less complexity. Steel rope is wound around the tire. The radius of the tire is called as moment arm in this study. Torque that obtained from tension spring can be manipulated as desired by changing the tire radius. This gives flexibility on the spring constant.

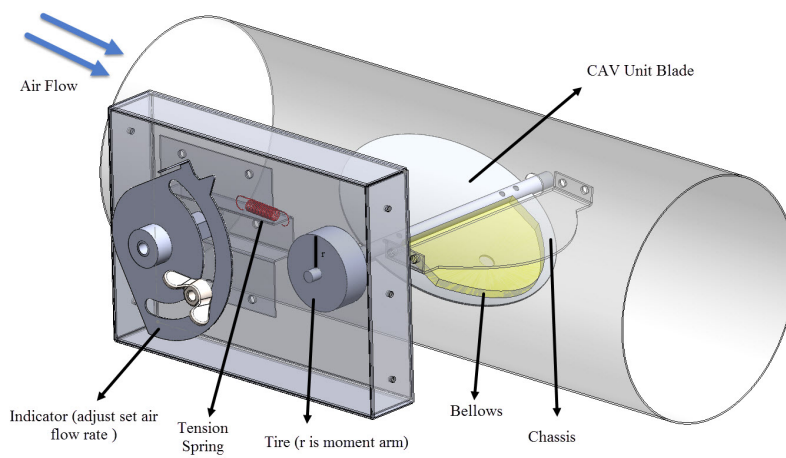


Figure 2.19: CAV Unit Design



## 2.4.1 CAV Unit Components

CAV unit consists of 3 main parts namely air duct, blade and control box. These parts are shown Figure 2.20.

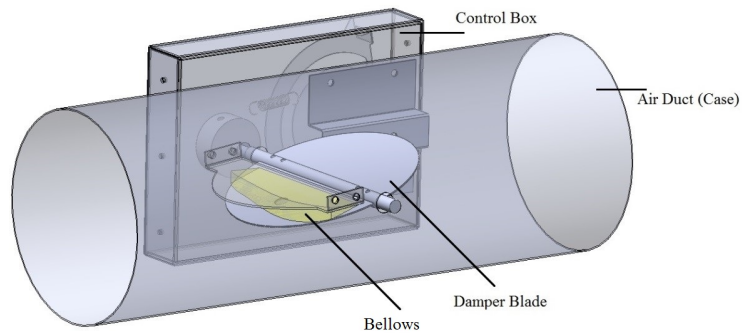


Figure 2.20: Parts of CAV Unit

### 2.4.1.1 Air duct (Case)

Case holds all the parts of the CAV unit. It is designed to minimize air leakage. In order to prevent the air leakage rubber gaskets are used on the both ends of the CAV unit so it fits tightly in to the air duct system and it maintains air duct continuity. Thus, this minimizes leakage.

### 2.4.1.2 CAV Unit (Damper) Blade

The second part is CAV unit blade. Blade is one of the most important elements of CAV unit. It regulates air flow rate by changing resistance of CAV unit for “right” amount. Damper blade is the part that limits the air flow rate by closing or opening the air flow area. Blade also holds the bellows which absorbs excessive oscillations on the blade.

### 2.4.1.3 Control Box

The third part of the CAV unit is control box. Main purpose of it is adjusting the desired air flow rate. In other words, how much air flow rate pass through CAV unit is determined by control box. To adjust higher air flow rate, pretension of the tension spring is increased.

One end of tension spring is connected to tire and the other end of the spring is connected to indicator via steel rope. Tire is tightly mounted to shaft which holds CAV unit blade so change in the blade angle changes tension spring length. Desired air flow rate can be set by rotating the indicator. When desired air flow set butterfly screw is tightened to fix indicator position. Close view of designed control box can be seen in Figure 2.21.

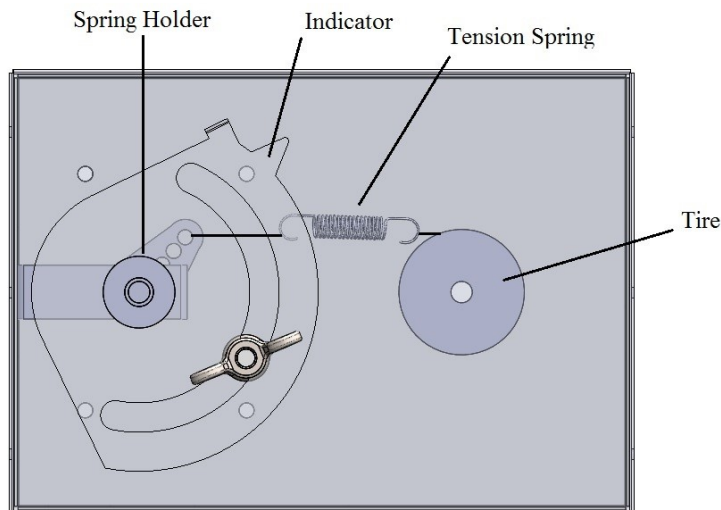


Figure 2.21: Control Box for CAV Unit

Final version of control box for CAV unit can be seen in Figure 2.22. Air flow rate can be set for desired value. When indicator is rotated in counter clock wise direction air flow rate can be increased because this motion introduces pretension to spring.

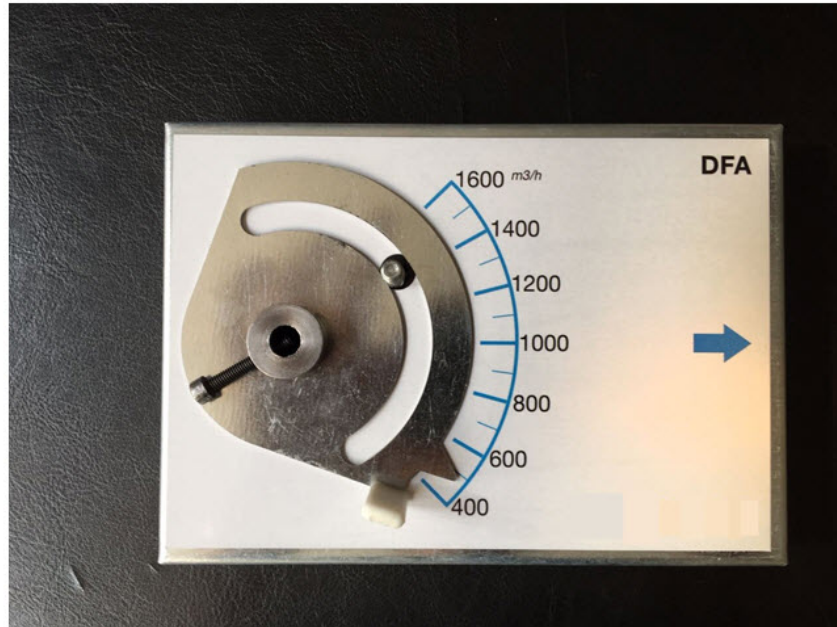


Figure 2.22: Final Version of Case of Control Box



## CHAPTER 3

### CFD ANALYSES OF CONSTANT AIR VOLUME (CAV) UNIT

#### 3.1 General Information and CFD Integration

Basic flow equations can be easily solved by almost any computer thanks to technological developments. Engineers begin to perform numerical experiments to reduce test cost and time. Computational fluid dynamics (CFD) methods are developed for these purposes. In the market there are many CFD codes available to solve 3D Navier-Stokes equations numerically. By these powerful codes and available commercial CFD programs design processes are shortened significantly. In addition, velocity profiles, pressure distributions, moments, streamlines etc. can be monitored by CFD programs. In laboratory environment, they can be observed with highly advanced and expensive devices.

A design engineer can perform numerical experiments to validate his/her design by using CFD programs. In this study, FLUENT is used to analyze CAV unit design. CFD integration into design phase provides early awareness about design errors. Since designed CAV unit is on the computer environment, error correction is very easy. In this study, CFD analyses are performed in order to see aerodynamic torque on the blade and pressure drop over CAV unit. Moreover, flow features inside the CAV unit can also be visualized by using CFD program.

## 3.2 CFD Analyses

CAV unit is analyzed by commercial CFD program which is FLUENT. Air flow inside of CAV unit is modeled. High turbulence regions and vortices after CAV unit blade are calculated and they are visualized by streamlines. Pressure difference over CAV unit and moment over the CAV unit blade is calculated. Analyses details are explained in the following sections.

### 3.2.1 Simplified CAV Unit Geometry

In order to manufacture CAV unit, all the details of it should be clearly specified in 3D solid model. However, this solid model has to be simplified for CFD analyses. Small parts are deleted to avoid meshing very small regions and also they are not expected to have crucial influence on the flow through CAV unit. For example, shaft that holds the blade, nuts and screws are not modeled. 3D solid model of CAV unit is created by SolidWorks. Blade angle can be easily changed by using this program and changing blade angle is essential to this study. Therefore, SolidWorks CAD program is selected. After drawing simplified geometry, extraction of fluid volume is needed to perform CFD analysis in Fluent. For this purposes Ansys Space Claim modeling program is selected. Fluid volume extraction is one of the best features of this program. In Figure 3.1. simplified and modified CAV unit geometry is given. Air flow inlet is labeled as "inlet", outlet of air flow is labeled as "outlet".

Analyzed CAV unit has 160 mm outer diameter. Blade has a thickness of 1 mm. In reality whole length of the CAV unit is 320 mm. However, in order to eliminate unwanted effect of reverse flow overall CAV unit is extended. It is 1.92 meters which corresponds to 12 diameters. This length is divided by 2 diameters for upstream part and 10 diameters for downstream part which can be shown in Figure 3.2. This length determination is also studied by Henderson [14]. After the geometry simplification and modification, fluid volume is extracted.

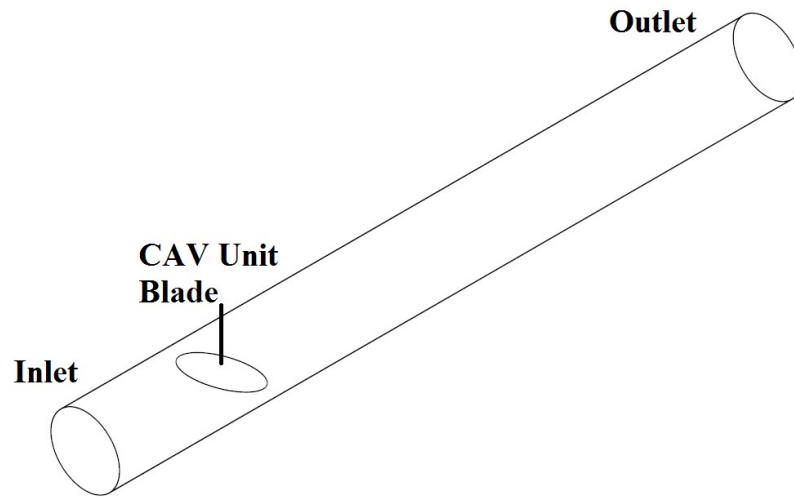


Figure 3.1: Simplified CAV Unit Geometry

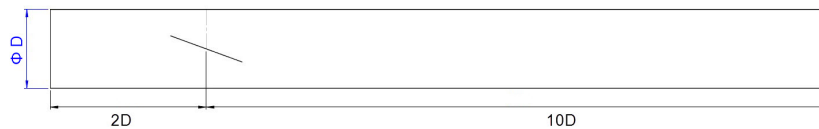


Figure 3.2: Geometrical Details of 3D CAV Unit Used for CFD Analyses

### 3.2.2 Meshing

Meshing has significant importance to obtain reliable results. Mesh consists of nodes and elements. Basically, high mesh numbers give better results. However, high numbers of mesh require more time and more computational power. Moreover, after certain mesh size is reached, the solution is not effected by the mesh size which is called mesh independency. Therefore, mesh number should be high enough to give good results and less enough to obtain solutions in a reasonable time period.

Meshing program of ANSYS software is used to construct grids. Even though, this program has automatic meshing feature, user defined meshing procedure is preferred. Hexahedral elements can give the same result with low number of element when it is compared to tetrahedral elements. Therefore, some modification is done in order to increase hexahedral elements. Simplified geometry is divided into 3 parts. Upstream and downstream parts are meshed with hexahedral elements. Middle part or blade part is meshed with tetrahedral elements. Since behind the blade is highly turbulent, outlet

part element size is finer than inlet part element size. Total number of hexahedral element is about 2 millions. Blade part is meshed with tetrahedral elements. Total tetrahedral element number is about 2 millions. Total number of elements in this CFD analysis is about 4 millions. Grids are constructed for 10°, 20°, 30°, 40° blade angles. In Figure 3.3. section view of meshed geometry is given. Additionally, in Figure 3.4 close view of the blade part meshes is given.

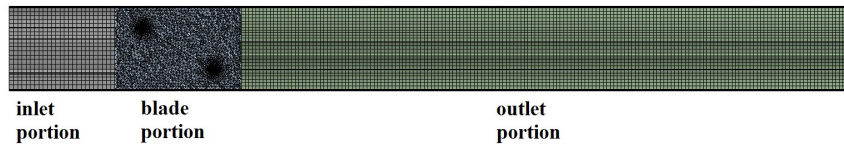


Figure 3.3: Section View of 3D Geometry of Generated Mesh

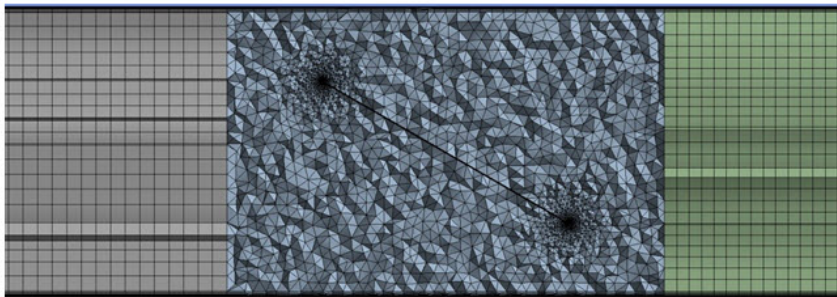


Figure 3.4: Close View of the Blade Part Mesh

In order to achieve mesh independency different size grids are generated. Results in Figure 3.5. show that even if mesh size increased from two millions to four millions analysis result changes only 0.3 percent which means mesh independency is achieved.



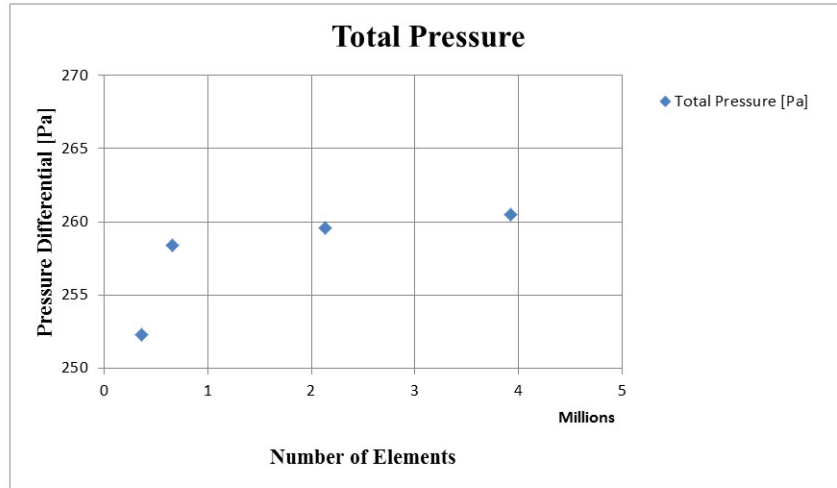


Figure 3.5: Analysis Results for Different Number of Elements for 160 mm CAV Unit for 600 m<sup>3</sup>/h

### 3.2.3 Boundary Conditions

For the CFD analyses of the CAV unit, two different flow boundary conditions can be applied. One is pressure inlet, pressure outlet and the other one is velocity inlet, pressure outlet. First method requires more time to achieve convergence criteria because in every iteration flow rate and pressure changes. However the second method, gives results faster because flow rate does not change. The analysis are performed according to inlet air velocities of 5.5 m/s, 6.9 m/s, 8.3 m/s which are correspond to 400 m<sup>3</sup>/h, 500 m<sup>3</sup>/h, 600 m<sup>3</sup>/h air flow rates respectively. At the outlet region, pressure outlet boundary condition is used and it is set to 0 Pa since operating condition is 1 atm. Blade surface and air duct surfaces are indicated as wall with no slip boundary condition. Operation of CAV unit can be assumed as steady. Because, blade reacts pressure changes almost immediately and it stays still until system pressure changes. Therefore, for any blade angle, steady state solution can be obtained. A quasi-steady modeling approach is adopted in this thesis, where steady flow solutions are obtained at various blade angles [14]. Turbulence model selected as standard k- $\epsilon$  model since flow is fully turbulent. k- $\epsilon$  model is also used widely in the industry because of its robustness, accuracy and low computational cost [20]. As a solution method upwind scheme and SIMPLE algorithm are selected. For this analysis, they seem to be more stable according to literature [21]. SIMPLE algorithm is a predict and correct type

method. SIMPLE algorithm relates continuity equation and pressure correction equation. By using pressure correction equation, SIMPLE algorithm solves for pressure and velocity values [20].

### 3.3 CFD Analyses Results

As convergence criteria following are accepted. Pressure difference between successive iterations should be less than 1% for the last 10 iterations. In Figure 3.6. convergence history of inlet pressure is given.

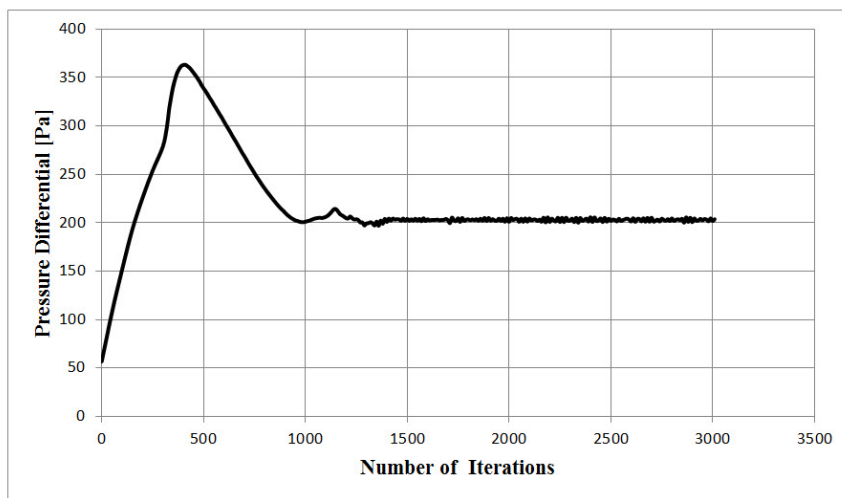


Figure 3.6: Convergence Plot for 500 m<sup>3</sup>/h and 40 ° Blade Angle

For non-zero blade angles formation of two counter rotating swirling vortices are common and it is observed in the downstream which can be seen in the Figure 3.7. Incoming flow hits the blade and pressure difference over the blade pushes air downward near the edges and creates swirling flow. This behavior is also noted by Henderson [14]. Toro et al [22] also noted the presence of a strong pair of vortices behind the blade.

CFD analysis results for moment on the blade for various air flow rate and different blade angles can be seen in Figure 3.8. Moment and blade angle relation can be accepted as linear.

CFD analysis results for pressure difference between inlet and outlet of CAV unit for

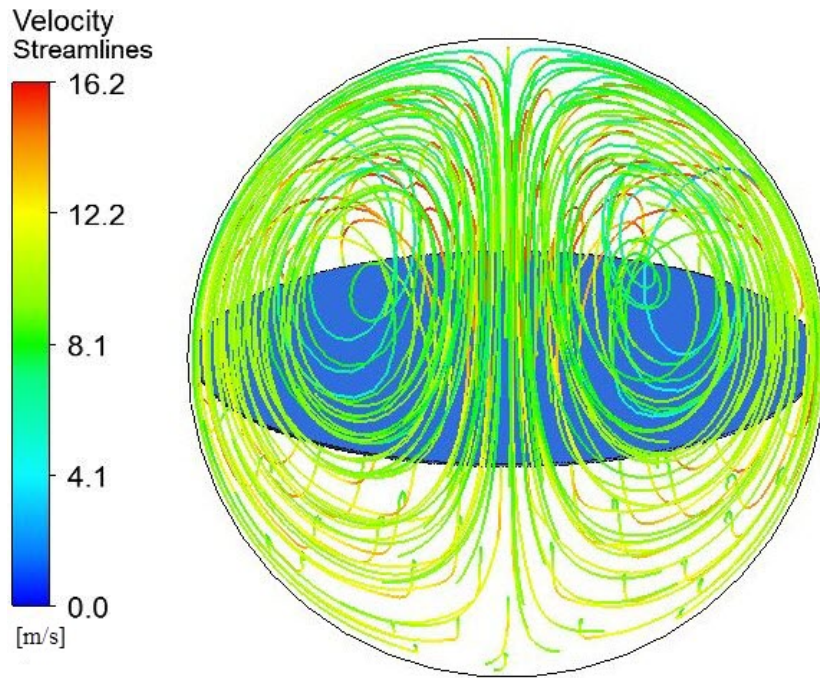


Figure 3.7: Velocity Streamlines at the Downstream for the Blade Angle  $40^\circ$  for  $500 \text{ m}^3/\text{h}$

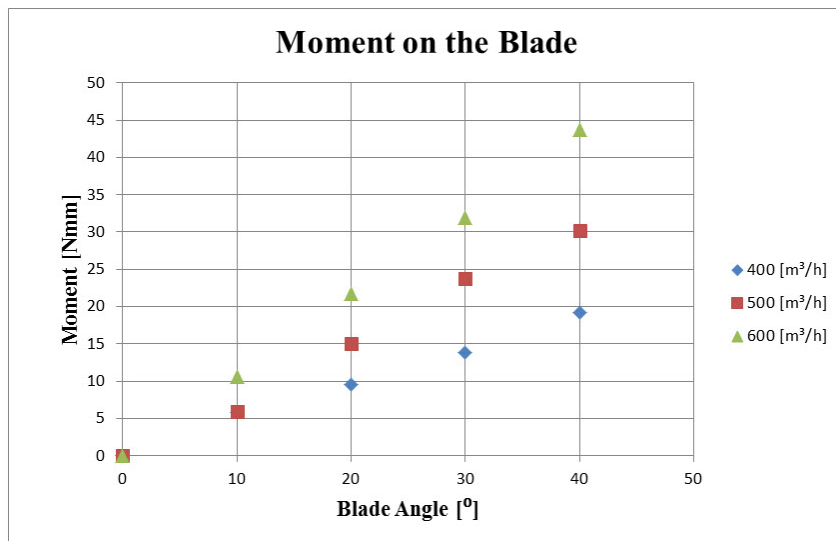


Figure 3.8: CFD Results for Moment and Blade Angle

different air flow rate and different blade angle can be seen in Figure 3.9.

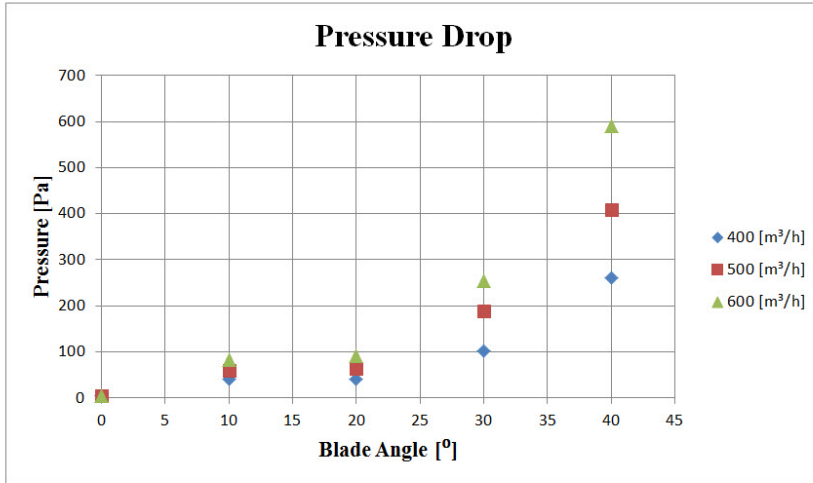


Figure 3.9: CFD Results for Pressure Drop and Blade Angle

Figure 3.9 can also be represented as pressure drop versus air flow rate plot which can be seen in Figure 3.10. Increase in the blade angle which, means that blade reduces the air flow area, causes the increase in pressure drop because resistance coefficient increases. Obtained curves almost perfectly fit the Equation 1.1.

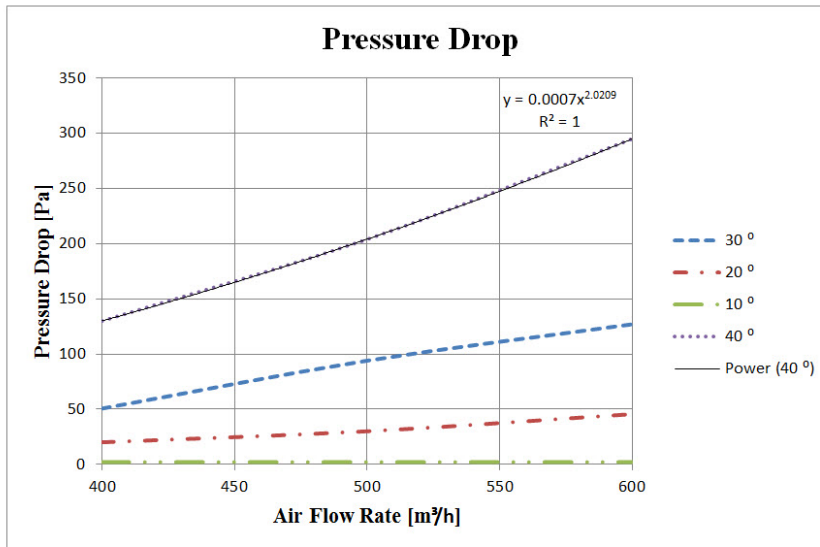


Figure 3.10: CFD Results for Pressure Drop and Air Flow Rate

Pressure distribution inside of the CAV unit is given in the following figures. Red color represents high pressure values and light blue color represents low pressure values. As expected high pressure region is located at inlet side of the blade and low pressure region is located at back side of the blade.

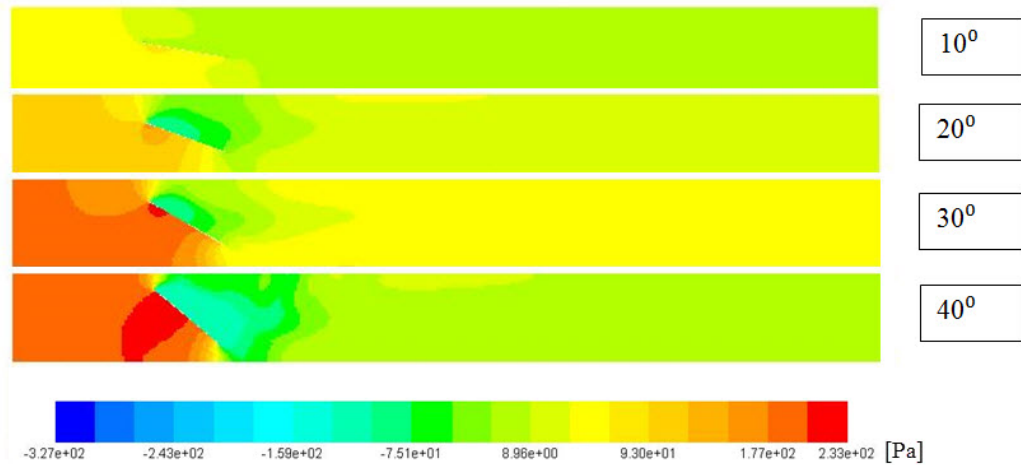


Figure 3.11: Pressure Distribution for Various Blade Angle with Flow Rate  $500 \text{ m}^3/h$

Velocity distribution inside of the CAV unit is given in the following figures. Red color represents high velocity values and blue color represents low velocity values. As expected higher velocities are located at small openings which is the region between blade and the CAV unit wall.

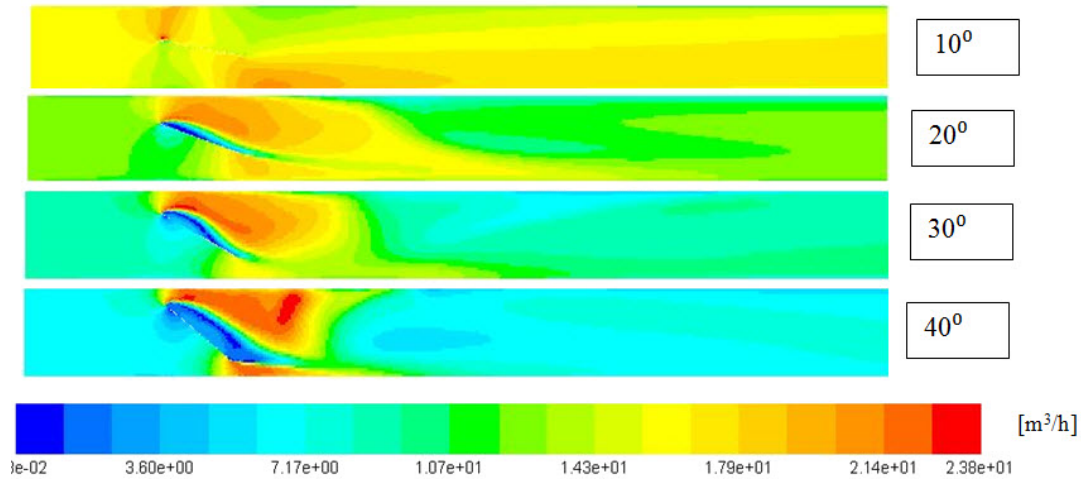


Figure 3.12: Velocity Distribution for Various Blade Angle with Flow Rate  $500 \text{ m}^3/h$

### 3.3.1 Comparison of Theoretical and CFD Results

In Chapter 2, pressure drop and moment are calculated according to 2D mathematical model. In Figure 3.13, pressure drop results are compared. Nonlinear relation is captured by both hand calculation and CFD analysis. Moreover both results are in agreement for small blade angles. For high blade angles deviation between two solution increases. Main reason is that for high blade angle flow behind the blade is highly complex and 2D model is not adequate to model the region.

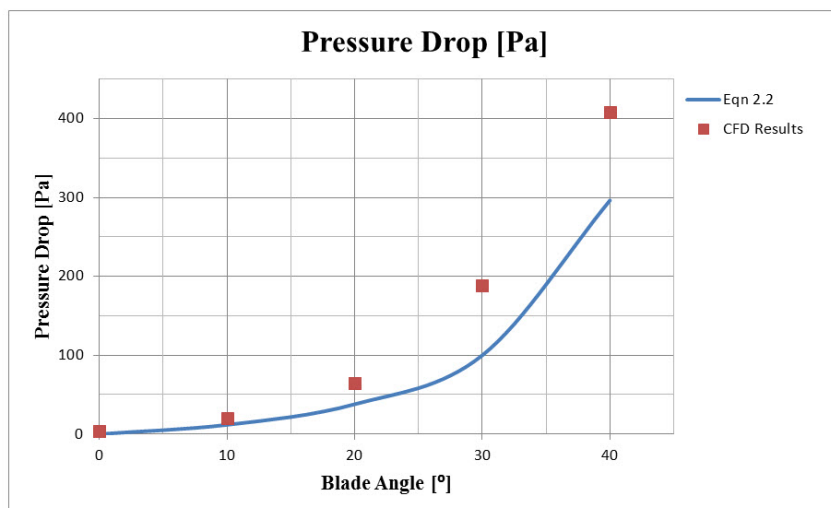


Figure 3.13: Eqn 2.2 and CFD Results Comparison for Pressure Drop Over CAV Unit

In Table 3.1. deviation between Equation 2.2. and CFD results are given.

Table 3.1: Deviation between Eqn 2.2 and CFD Results

Blade Angle [deg]	Eqn 2.2 [Pa]	CFD Results [Pa]	Deviation [%]
0	0	4	100
10	12	20	41.4
20	38	64	40.9
30	100	188	46.8
40	296	408	27.4

In Figure 3.14. moment results are compared. Hand calculation is the results of Equation 2.7. As seen in the figure aerodynamic moment is over predicted.

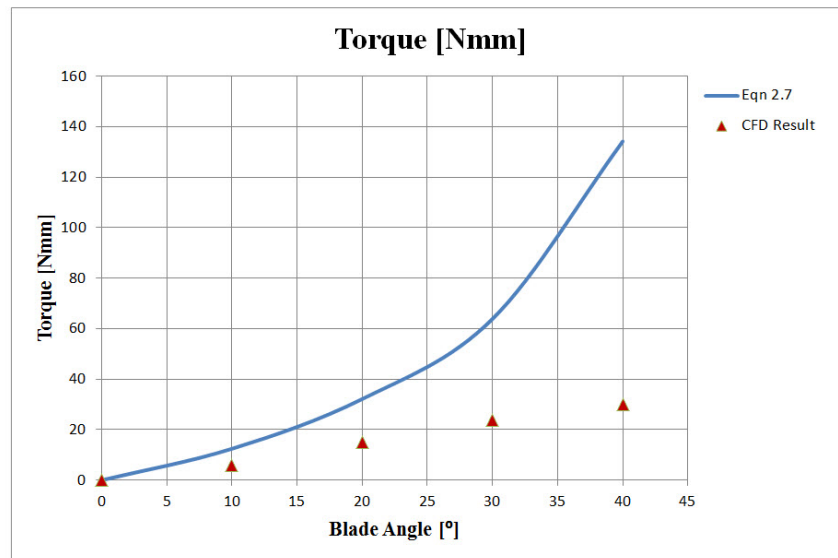


Figure 3.14: Eqn 2.7 and CFD Results Comparison for Moment Over CAV Unit Blade

In Table 3.2. deviation between Equation 2.7. and CFD results are given.

In Figure 3.15. moments due to tension spring is compared with CFD results. As seen in the figure predicted moment over the blade is very close to generated torque by the tension spring. Therefore, spring constant is predicted by using CFD results. Figure 3.15. is drawn by taking spring constant as 0.2 N/mm. This means that constant flow

Table 3.2: Deviation Between Eqn 2.7 and CFD Results

Blade Angle [deg]	Eqn 2.7 [Nmm]	CFD Results [Nmm]	Deviation [%]
0	0	0	0
10	12	6	100
20	32	15	113
30	64	24	166
40	134	30	346

rate can be obtained by using this specific tension spring for 160 mm diameter CAV unit. Performance results of this CAV unit is given in following chapter.

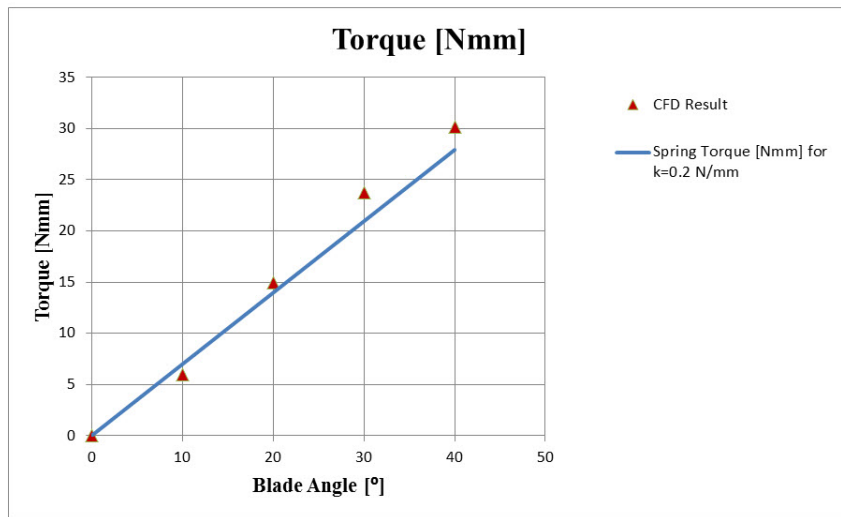


Figure 3.15: Predicted Spring Moment and CFD Results



In Table 3.3. deviation between spring moment and CFD results are given.

Table 3.3: Deviation Between Spring Moment and CFD Results

<b>Blade Angle [deg]</b>	<b>Spring Const. 0.2 N/mm</b>	<b>CFD Results [Nmm]</b>	<b>Deviation [%]</b>
<b>0</b>	0	0	0
<b>10</b>	7	6	17
<b>20</b>	14	15	7
<b>30</b>	21	24	13
<b>40</b>	28	30	7



## CHAPTER 4

### EXPERIMENTAL FACILITIES AND PERFORMANCE EVALUATIONS

In this chapter, experimental setup and test procedures are presented. Details of test setup are also explained. Designed CAV units are tested in research and development laboratory in Kes Klima. Full scale CAV units are tested which are in different diameters from 100 mm to 400 mm. In Figure 4.1 test setup can be seen. At the left hand side there is a fan unit which is connected to settling chamber via sheet metal duct. Settling chamber is at right hand side on the figure and it holds CAV unit which is the test item. This setup was used to measure pressure drop over CAV unit and aerodynamic torque on the CAV unit blade. Moreover, air flow rate and spring stiffness are also measured.



Figure 4.1: Test Bench

## 4.1 Test Setup

Tests are conducted in an open air circuit driven by a capacity of 15000 m<sup>3</sup>/h centrifugal fan and its speed is controlled by variable frequency drive. As affinity laws stated, fan flow rate can be increased or decreased by changing fan speed. Therefore, air flow rate supplied from fan unit can be changed. A schematic view of the whole experimental setup is shown in Figure 4.2.

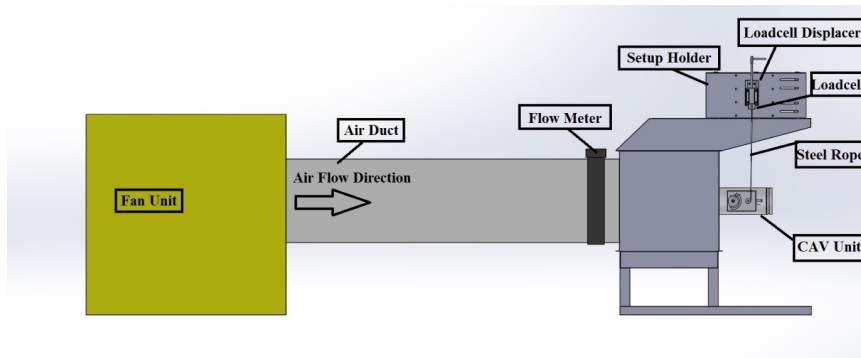


Figure 4.2: Schematic View of the Test Bench

In Figure 4.3. close view of test setup is given. CAV unit and moment measurement setup is mounted to settling chamber. Different diameters of CAV units can also be mounted to settling chamber with suitable adapters.

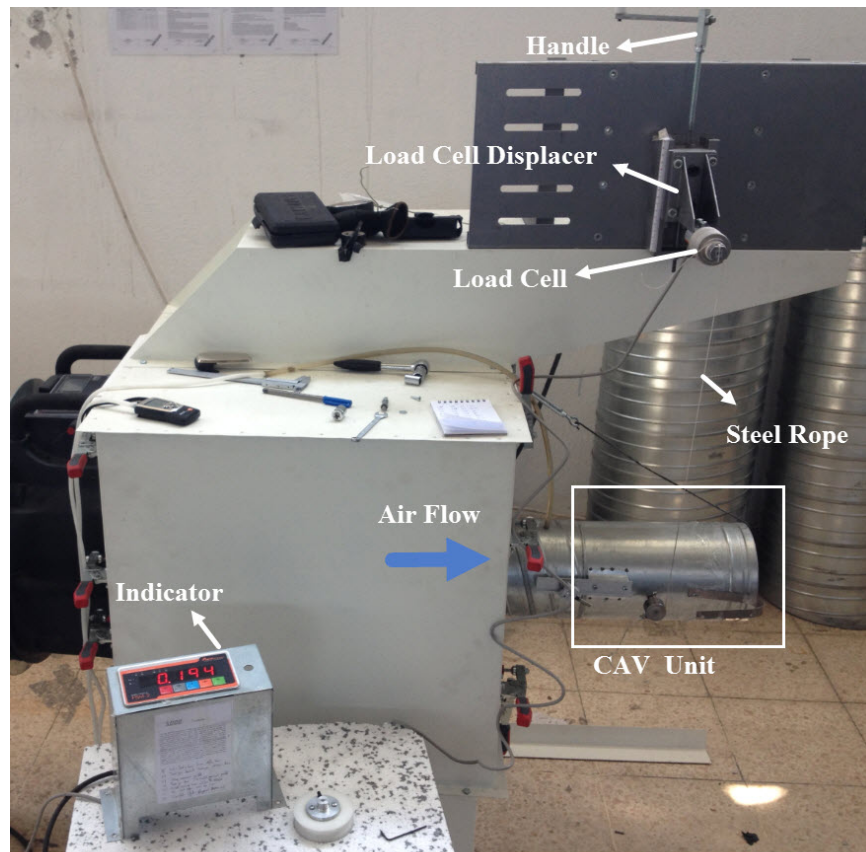


Figure 4.3: Close View of the Moment Measurement Setup

There exists a flow meter which is TSI Airflow Prohood at the entrance of the settling chamber. The flow meter is capable to measure air flow rate between  $42 \text{ m}^3/\text{h}$  to  $4250 \text{ m}^3/\text{h}$ . It has a  $\pm 3 \%$  of reading and  $\pm 12 \text{ m}^3/\text{h}$  flow rate measuring accuracy. Loadcell and loadcell displacer is mounted to test setup in order to measure aerodynamic torque on the CAV unit blade. In Figure 4.4. CAV unit blade angle measurement setup is shown. Pointer shows blade angle.

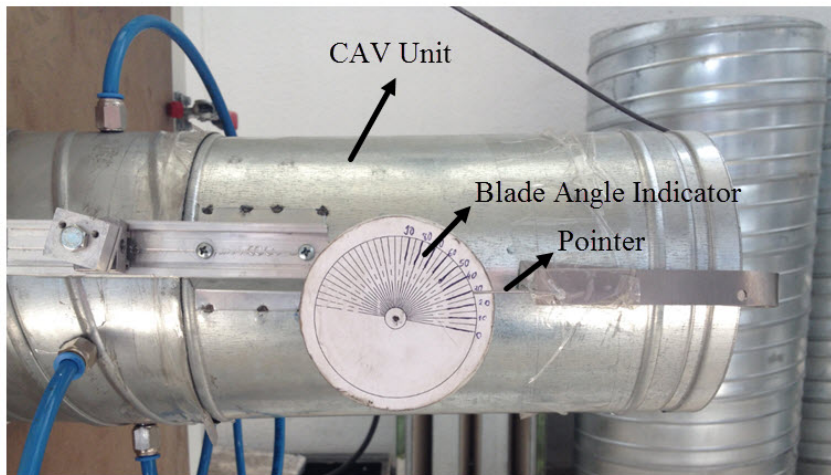


Figure 4.4: CAV Unit Blade Angle Measurement

Testo manometer can be seen in Figure 4.5 which is used to measure inlet pressure of CAV unit.

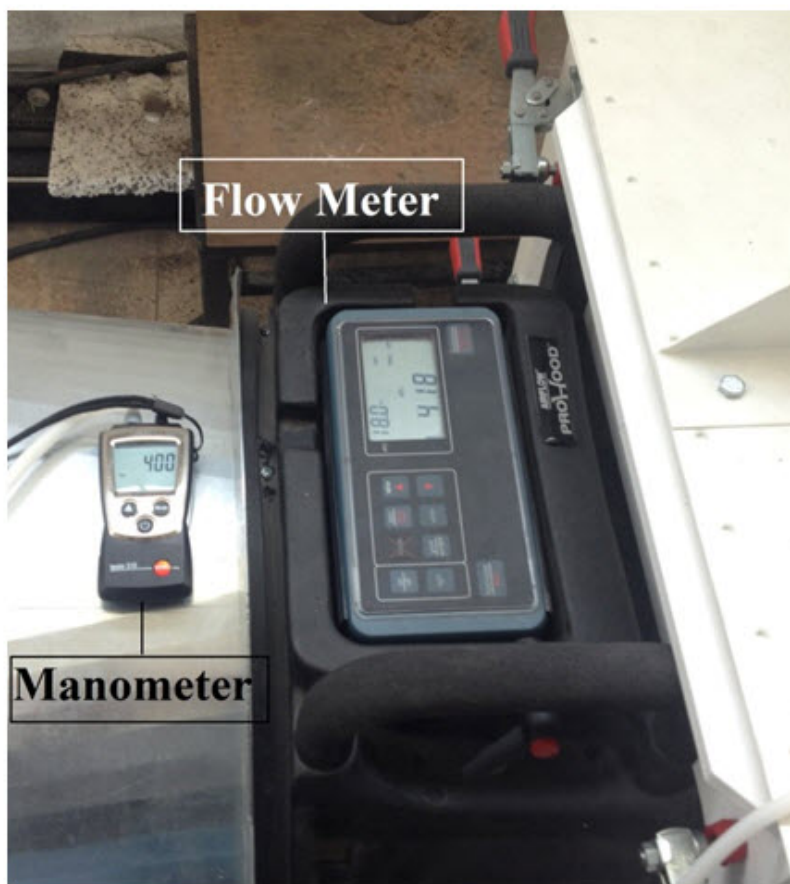


Figure 4.5: Manometer and Flow Meter

## 4.2 Calibration of Test Instruments

In order to obtain reliable results, measurement devices have to be calibrated. Pressure transducer, hot wire anemometer, and flow meter need not to be calibrated since they are bought during thesis study and these devices are calibrated by their vendors. However, load cell should be calibrated because it was bought some time ago. In order to calibrate load cell, 1288 grams dead weight is used which is shown in Figure 4.6.



Figure 4.6: Dead Weight

Calibration procedure of the loadcell is as follows. First, dead weight is connected to the loadcell by means of a steel rope which has a negligible weight as seen in Figure 4.7. Then, known dead weight value is entered manually to the loadcell indicator controller. Next, zero calibration is also done. When nothing is attached to the load cell, indicator is set to zero by pressing the "Zero" button on the controller. This is the calibration procedure for load cell according to two known values [23].

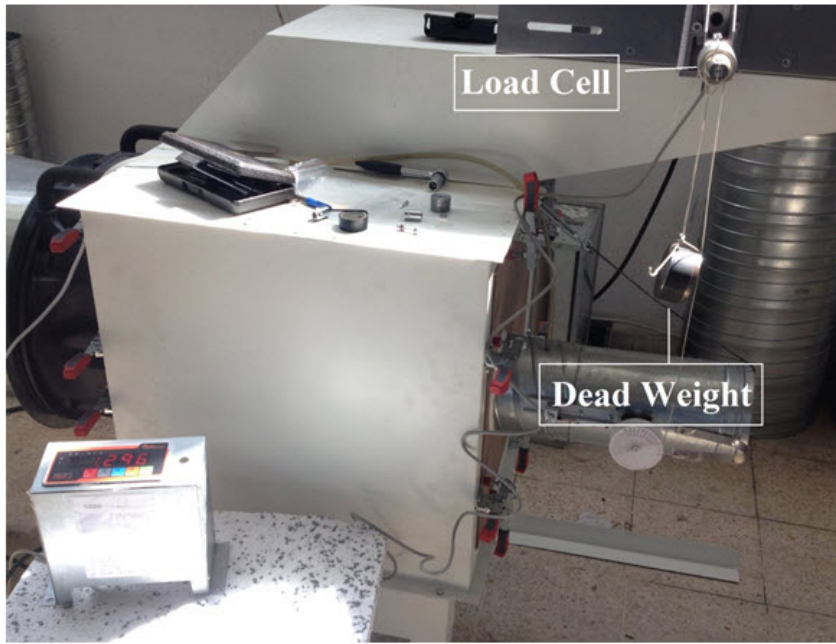


Figure 4.7: Load Cell Calibration

### 4.3 Uncertainty Analysis

Uncertainty is unavoidable part of engineering. When a measurement is made, it contains some errors and there is always some difference between the measured value and the actual value. However, if the amount of uncertainty can be determined, measured values can be used with confidence.

This experimental setup contains some error sources. Ambient temperature affects flow meter measuring but it is close to  $20C^{\circ}$  throughout the study so temperature effects are neglected. Air leakage from ducts and mounting interfaces is almost inevitable and its amount can not be exactly known but some precautions are taken. Silicon and sponge strips are applied to possible air leakage locations in order to reduce air leakage as much as possible. Air flow rate is measured with TSI Airflow Prohood flow meter. Its uncertainty is stated as  $\pm 2\%$  of reading at  $20C^{\circ}$  and 1013 mb [24].

Pressure measurements are done by using Testo 510 pressure transducer. Its measuring accuracy is  $\pm 1 + 1.5\%$  of reading. This means that for 1000 Pa the error is 16 Pa



which is acceptable for this study[25].

Air velocity is measured by Extech SDL350: Hot Wire CFM Thermo-Anemometer. Uncertainty of this device is  $\pm 5\%$  of reading. Since maximum air velocity is 10 m/s, error is 0.5 m/s and it is acceptable for this thesis [26].

Puls BT beam type loadcell is used to measure torque on the CAV unit blade. The device has  $\pm 1$  gram accuracy in full scale output.

#### **4.4 Laboratory Measurements**

In this study, 4 main measurements are done namely pressure drop measurement over CAV unit according to different blade angles, moment measurement of CAV unit blade for different air flow rates and different blade angles, measurement of spring constants of tension springs and measurement of air velocity at the exit plane of CAV unit. Details of these measurements are explained in the following sections.

##### **4.4.1 Pressure Drop Measurement**

Pressure drop over CAV unit is measured by using an experimental setup which is shown in Figure 4.8. The aim of pressure measurement is monitoring pressure drop over CAV unit according to various blade angles for constant air flow rate. This information is used to correlate blade angle and pressure drop for different flow rates. Moreover, obtained pressure values are used to validate CFD codes. This setup is designed to obtain the most reliable results as possible. Inner duct surface of the test setup is smooth and free from irregularities. Static pressure measurement ports are located at the duct wall so the velocity of the air stream does not influence the pressure measurement. Static pressure measurement ports are located according to ASHRAE standard 111-1988 [27]. Differential pressure values are read from Testo 510 differential pressure transducer. This device has a measuring range from 0 to 10000 Pa gage pressure with accuracy of  $\pm 3$  Pa. Sampling rate of this instrument is two samples per second which is enough to supply adequate measurement results.

Upstream pressure is measured from inlet plane of the CAV unit and from four different location which are  $90^\circ$  apart from each other. These four pressure ports are connected to a main tube[28]. Then this tube is attached to (+) side of the manometer. (-) side of the manometer is not connected to any tube it is leaved open, because the CAV unit is opened to atmosphere. Therefore, the pressure value read on the manometer is the differential pressure or pressure drop between upstream and downstream of CAV unit. Moreover, CFD validations are done according to these measured differential pressure values.

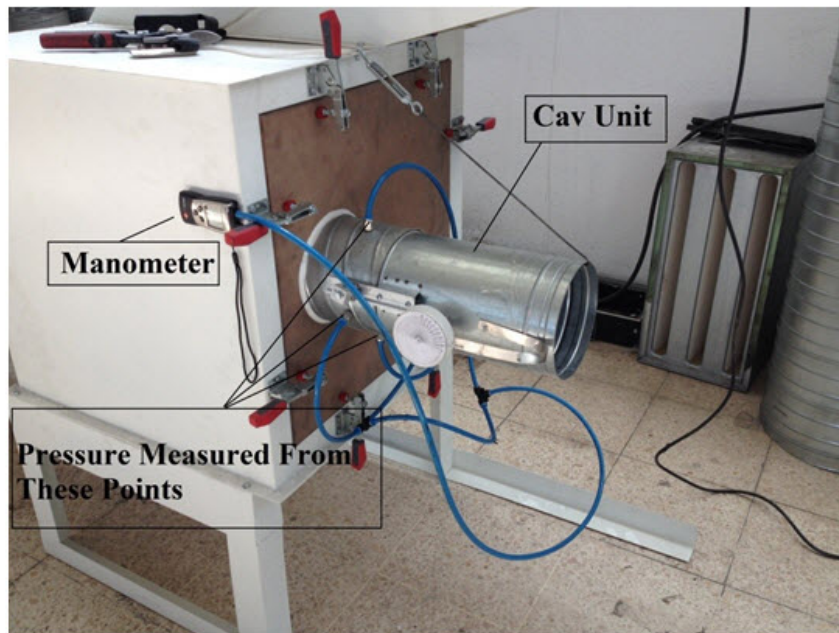


Figure 4.8: Pressure Drop Measurement Setup

Pressure measurements are performed for 3 different air flow rates which are  $500 \text{ m}^3/\text{h}$ ,  $600 \text{ m}^3/\text{h}$ ,  $700 \text{ m}^3/\text{h}$  and different CAV unit blade angles.

#### 4.4.1.1 Pressure Drop Measurement Procedure

In order to measure differential pressure over the CAV unit following procedures are applied.

1. CAV unit blade is set to desired angle (for example,  $10^\circ$ ) by means of a clamp and angle-paper which shows blade angle from horizontal.

2. Fan flow rate is set to desired flow rate (for example, 500 m<sup>3</sup>/h) and it is constant for whole measurement.
3. Pressure value is read from pressure transducer and it is recorded to data sheet.
4. CAV unit blade is set to new angle which is 10° more from previous angle.
5. Due to increase in the blade angle, supplied air flow rate from fan decreases. Fan speed should be increased by using variable frequency drive until set air flow rate at the second step is reached.
6. Pressure value is read from manometer and it is recorded to data sheet.

#### **4.4.2 Bellows Pressure Measurement**

As a damping unit inflatable bellows is selected. The aim of this measurement is to observe how bellows pressure changes according to different blade angles. For different angles different pressure values are measured at the bellows.

Same procedure is followed for measuring pressure differential over the CAV unit which is explained in previous section. Two manometer is used for this measurement. One of the them is connected to inlet port of the bellows on the CAV unit blade and this location is stated as "bellows pressure measurement port" in Figure 4.9. Bellows inlet pressures are measured for different blade angles with 5 degrees increments and different air flow rates. The other manometer is connected to inlet side of the CAV unit and pressure differential is measured. Close view of the setup is shown in Figure 4.10.

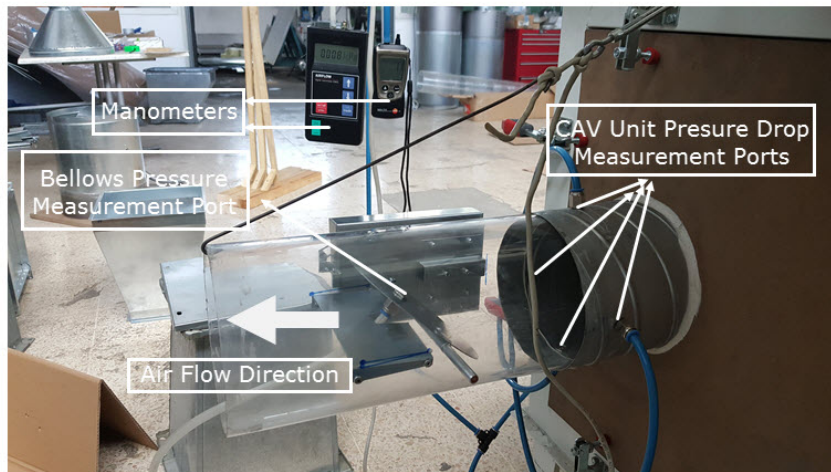


Figure 4.9: Measurement of Bellows Pressure

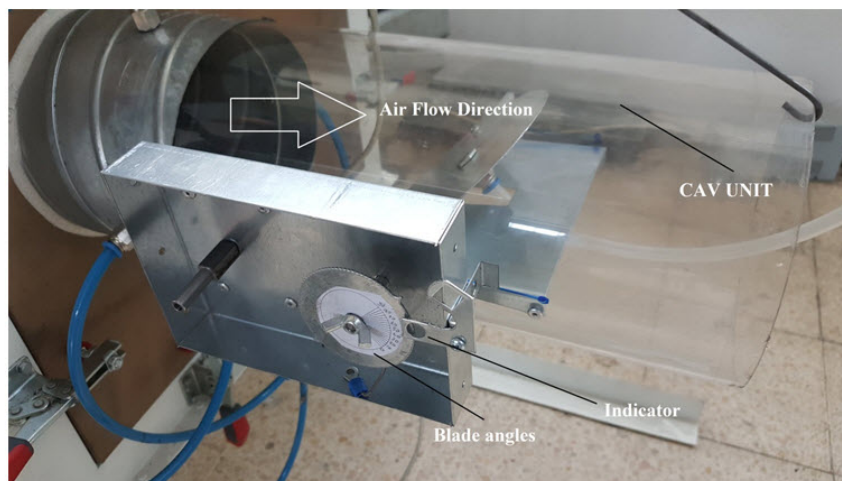


Figure 4.10: Close View of the Setup

Bellows inlet pressure measurement is done for  $\phi$  160 mm diameter CAV unit.

#### 4.4.3 Measurement of Moment on the CAV Unit Blade

The purpose of this measurement is to determine torque on the CAV unit blade due to aerodynamic forces. Measured torque values are used to calculate spring constant and choose appropriate tension spring.

Moment measurement needs a special care to get reasonable results. To be able to measure the torque on the blade moment measurement setup is designed and manu-

factured. In Figure 4.11 designed test setup can be seen.

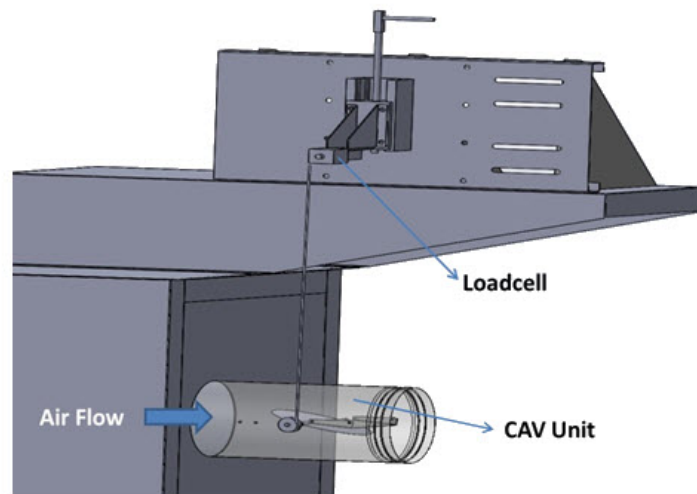


Figure 4.11: Measurement of Moment on the Blade Setup

In this setup, Puls FSM-2 weight indicator is used. This indicator converts signals that come from load cell to weight in grams. It has a sampling rate of 200 Hz and measuring range is 0-40 mV. In order to measure weight Puls BT series bending beam load cell is used. Measuring capacity of it is 10 kg. Average output error is  $\pm 1$  gram.

In Figure 4.12 details of the experiment setup is shown. In coming flow creates torque on the blade and blade tries to rotate in clockwise direction. Since blade is attached to a moment arm and it is connected to load cell via steel rope, force can be measured due to deflection on the load cell. Output of the load cell is weight in gram. To obtain force, weight value is multiplied by gravitational acceleration. Furthermore, torque value is measured by multiplying force value by moment arm.

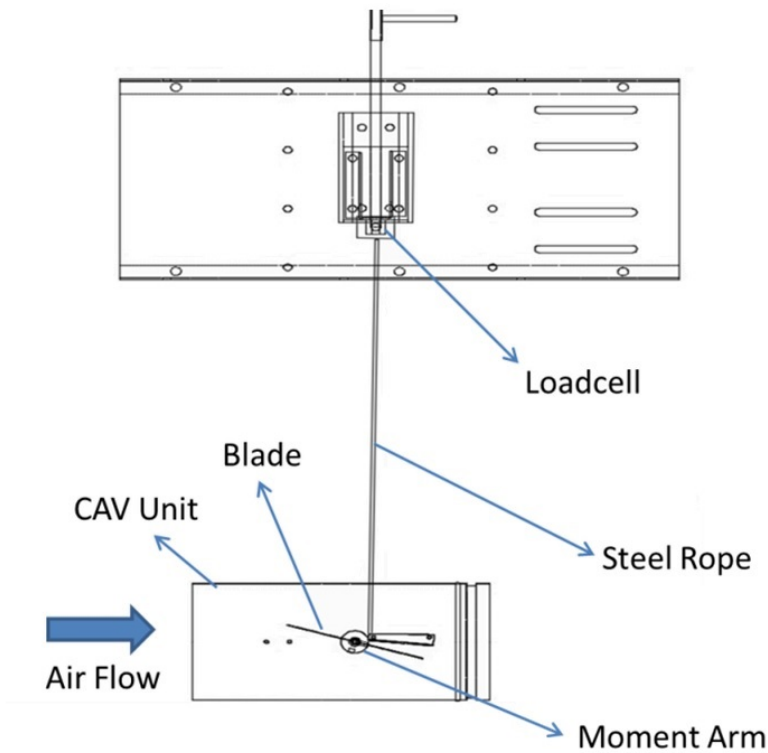


Figure 4.12: Details of Moment Measurement Setup

#### **4.4.3.1 Moment Measurement Procedure**

Moment measurement on the CAV unit blade is done according to following steps.

1. Load cell mounted to experiment setup.
2. One end of steel rope is attached to load cell and the other end of the steel rope is connected to moment arm. Note that moment arm is connected to the CAV unit blade and it cannot rotate independently.
3. CAV unit blade is set to desired angle by changing load cell position. (For example,  $10^\circ$ ). Note that blade is free to rotate from  $0^\circ$  to  $10^\circ$ .
4. When blade is at the desired angle, weight indicator is set to 0 gram.
5. Fan flow rate is set to desired flow rate and it should be constant for whole measurement.
6. Read and record the value shown by weight indicator.
7. Change the blade angle and follow the step 5 and step 6.
8. Multiply recorded data with gravitational acceleration to obtain force and multiply this value with moment arm to obtain torque on the blade due to aerodynamic forces.

#### **4.4.4 Spring Constant Measurement**

Spring stiffness or spring constant should be determined to be able to validate design calculation. Test item is tension spring. It is expected to have constant stiffness. Some of the devices that are used in this experiment setup are identical with the moment measurement setup. In addition these devices a caliper is used to measure spring elongation. Spring constant measurement setup can be seen in Figure 4.13.

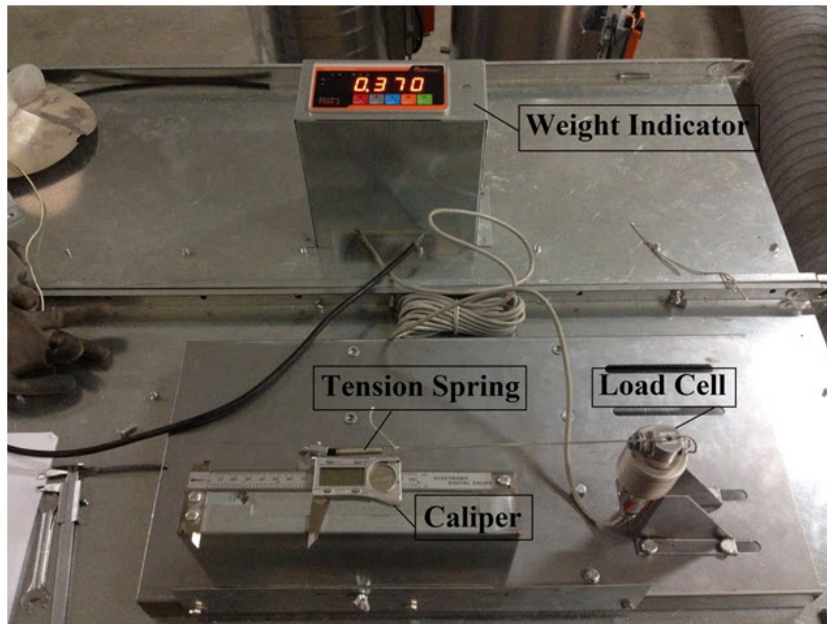


Figure 4.13: Spring Constant Measurement Setup

#### 4.4.4.1 Spring Constant Measurement Procedure

Spring constants are measured according to following steps.

1. Fix load cell to holder.
2. Attach one end of steel rope to load cell and the other end to the tension spring.
3. Mount tension spring to the caliper.
4. While spring is unstretched set indicator value to zero.
5. Move caliper 1mm and record the value seen on the indicator.
6. Repeat step 5 until spring is fully stretched.

#### 4.4.5 Air Velocity Measurement

Air velocity is measured by hot wire anemometer. The operation of hot wire anemometer depends on the fact that the resistance of a heated wire changes with its temperature. As air flows over the element in the probe, the temperature of the element is



changed from that which exists in still air, and the resistance change is indicated as a velocity on the indicating scale of the instrument.

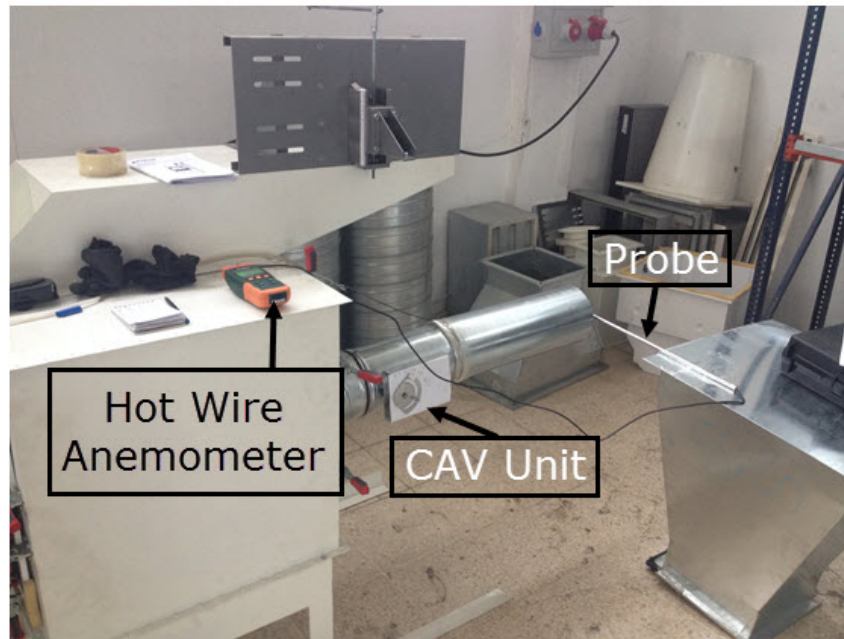


Figure 4.14: Air Velocity Measurement Setup

By measuring air flow velocity, CAV unit performance can be evaluated. Even though this measurement is not a main performance evaluation test, it can supply quick results. Aim of this measurement is that whether CAV unit supplies constant air flow rate or not. If the air flow velocity constant at the exit plane of CAV unit, air flow rate is also constant because exit area is constant. Air flow measurement is done with Extech SDL350: Hot Wire CFM Thermo-Anemometer/Datalogger. This device is capable of measuring air velocity between 0.2 m/s and 25 m/s. It has a resolution of 0.01 m/s and accuracy of  $\pm 5\%$  of reading. Features of this hot wire anemometer are enough to perform the measurement. Pressure drop is also recorded with differential pressure transducer during the air velocity measurement.

#### 4.5 Laboratory Measurements Results

Experimental results are given in this part of the thesis. Pressure measurement results, moment measurement results, spring stiffness determination results and air velocity

measurement results are given.

### 4.5.1 Pressure Measurement Results

In Figure 4.15 pressure measurement results for different blade angle are given in pressure drop versus blade angle graph. As seen in the figure increasing blade angle (which means decreasing air flow passage area) increase pressure drop. Additionally, for the same blade angle increasing air flow rate raises pressure drop.

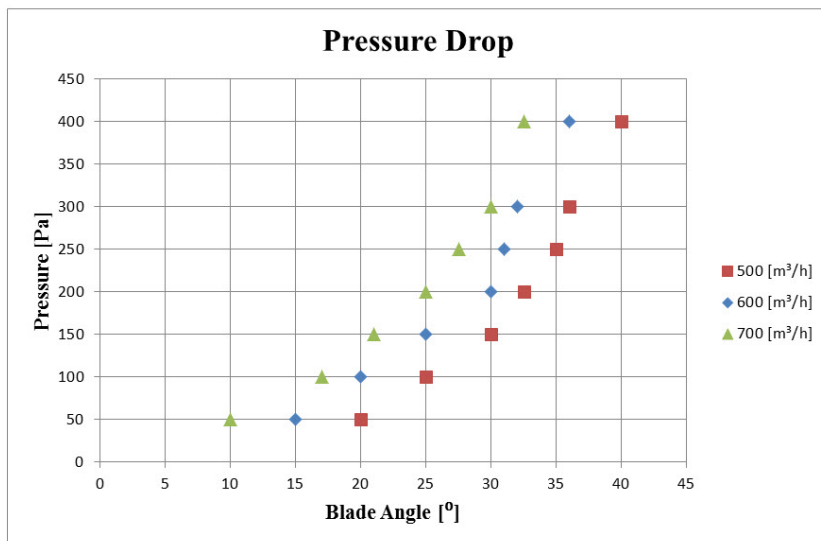


Figure 4.15: Pressure Drop Values for Different Flow Rates and Blade Angles

#### 4.5.1.1 Bellows Pressure Measurement Results

CAV unit pressure drop and bellows pressure comparison is given in Figure 4.16. Blade angle up to  $10^\circ$  bellows cannot be inflated because it is in vacuum. Up to  $40^\circ$  blade angle, there is a difference between pressure values. However this difference diminishes after  $40^\circ$  blade angle.

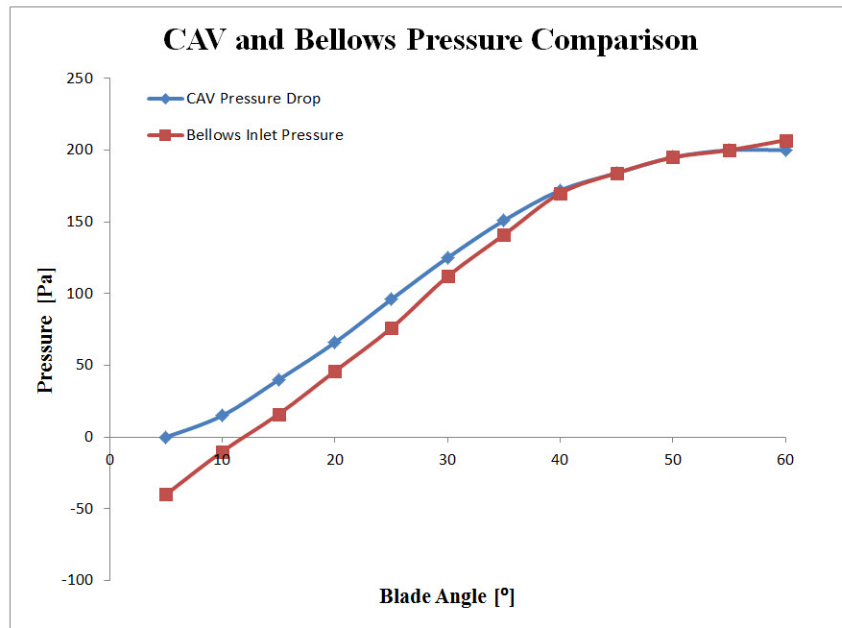


Figure 4.16: CAV Unit Pressure Drop and Bellows Inlet Pressure

#### 4.5.2 Moment Measurement Results

Figure 4.17 shows 160 mm diameter CAV unit blade torque measurement results according to different air flow rate. As seen, there is almost linear relation between blade angle and moment on the blade. Therefore, spring that has a constant properties can be used. Equation 2.12 is also predicted this relation.

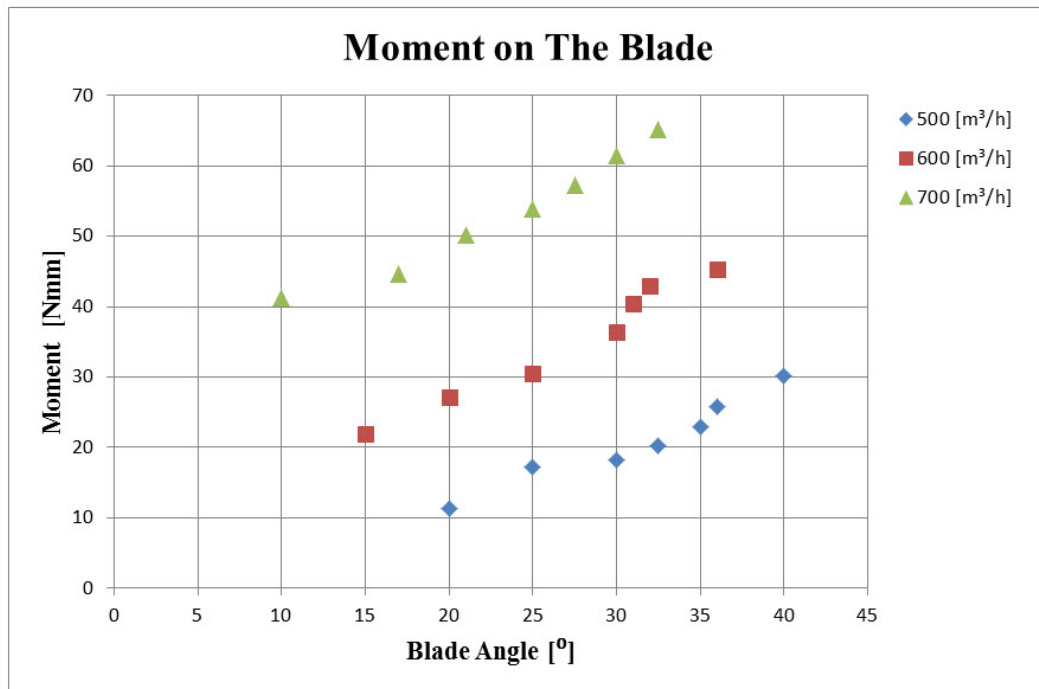


Figure 4.17: Torque on the CAV Unit Blade vs Blade Angle

### 4.5.3 Spring Constant Measurement Results

For different springs Figure 4.18 is obtained. As seen in the figure "spring 5" and "spring 6" practically are the same. "Spring 1" is the most stiff spring among the others because it gives maximum force for the same spring extension.

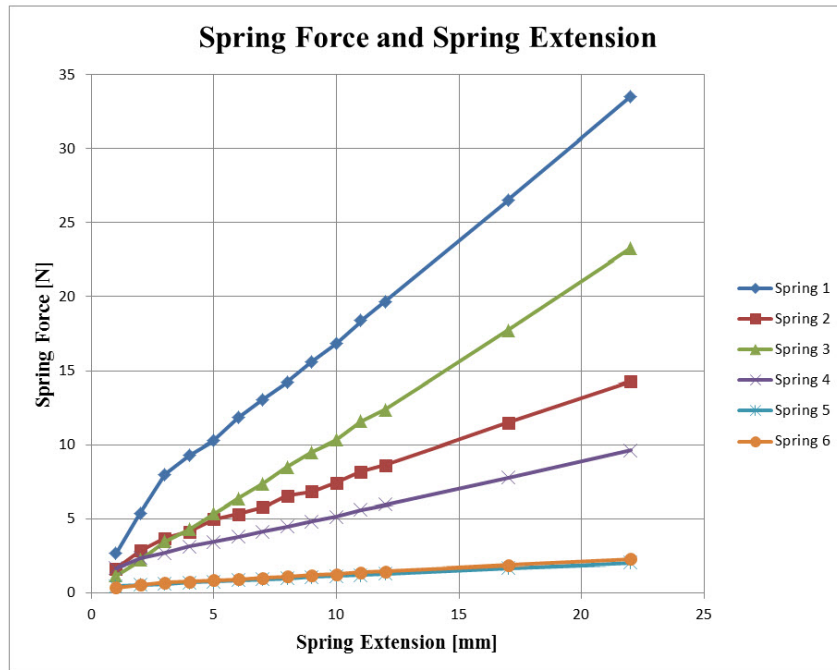


Figure 4.18: Spring Force values according to spring extensions

By using Figure 4.18 average spring constants can be calculated. Calculated spring constants are shown in Table 4.1 .

Table 4.1: Spring Constants

Spring	Spring Constant [N/mm]
<b>1</b>	1.714
<b>2</b>	0.9374
<b>3</b>	1.0724
<b>4</b>	0.7094
<b>5</b>	0.161
<b>6</b>	0.168

#### 4.5.4 Air Velocity Measurement

As seen in Figure 4.19 almost constant air velocity is obtained at the exit plane of CAV unit. This implies that flow rate is constant even if pressure drop increases.

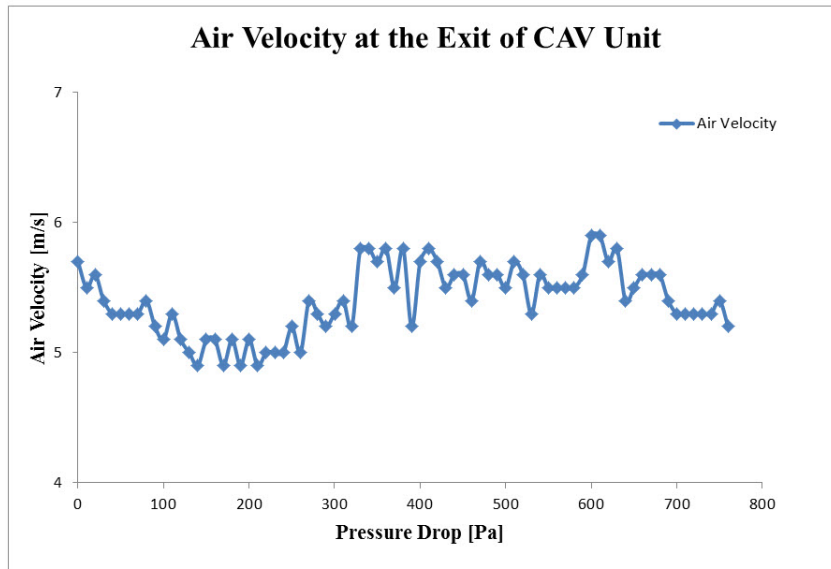


Figure 4.19: Variations of Air Velocity at the Exit Plane of CAV Unit

#### 4.6 Discussions for Laboratory Measurements

The following comments can be made on the experimental results.

1. Pressure drop and blade angle relation is nonlinear. Moreover, for same blade angle high flow rate causes high pressure drop.
2. Bellows pressure is negative up certain blade angle. Highest vacuum value is obtained when the blade angle is zero which means blade is parallel with ground.
3. Blade angle and torque on the blade can be assumed as linearly related according to measurement results and air flow controller will be designed according to this assumption.
4. Various springs are tested. As expected they all have constant stiffness.

5. Air velocity have a mean value around 5.5 m/s. Since measurement is done for only at a certain point at the exit plane of the CAV unit, air velocity value cannot be used for air flow rate calculation. However, it can be used to check supply of constant air flow rate.

#### **4.7 Performance Evaluations of CAV Unit**

After completing all numerical and laboratory experiments, CAV units are finalized. Performance test of 160 mm CAV unit for 543 m<sup>3</sup>/h is done and explained here.

As spring - tire combination 20 mm tire radius and "Spring 6" is selected according to design calculation result for 160 mm CAV unit and it is subjected to performance evaluation test. The procedure is as follows.

1. Mount 160 mm CAV unit to test setup tightly.
2. Set CAV unit air flow rate as 543 m<sup>3</sup>/h by using indicator on the control box.
3. Open flow meter and pressure transducer.
4. Start fan.
5. Increase fan speed by using variable frequency drive
6. Record pressure and flow rate
7. Repeat step 5 and step 6 until desired pressure range is covered.

In Figure 4.20, performance test of the CAV unit can be seen. Volumetric flow rate is set for 543 m<sup>3</sup>/h and  $\pm 10\%$  deviation is allowable around set flow rate value. Even if pressure differential increases as CAV unit operates, air flow rate stays in the limits. This indicates that CAV unit is successfully designed.

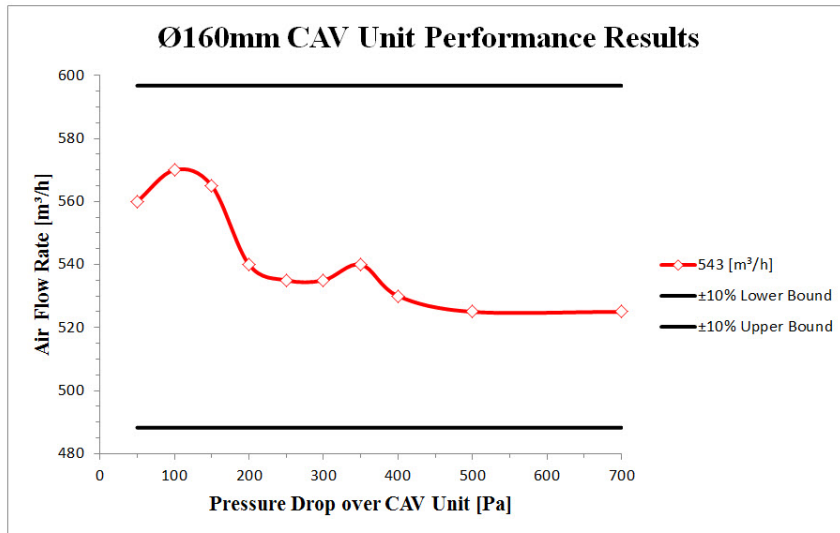


Figure 4.20: Ø160 mm CAV Unit Performance Result for 543 m<sup>3</sup>/h



## CHAPTER 5

### DISCUSSION AND CONCLUSION

#### 5.1 Discussion

Comparison between experiment and CFD analysis results is performed. Measured pressure values for specific air flow rate and blade angle are compared with calculated pressure values. In Figure 5.1 "Exp" represents experimental results and other lines stand for CFD analysis results. For 160 mm diameter CAV unit pressure values are compared for three different air flow rates and different blade angles. Both results are very close to each other.

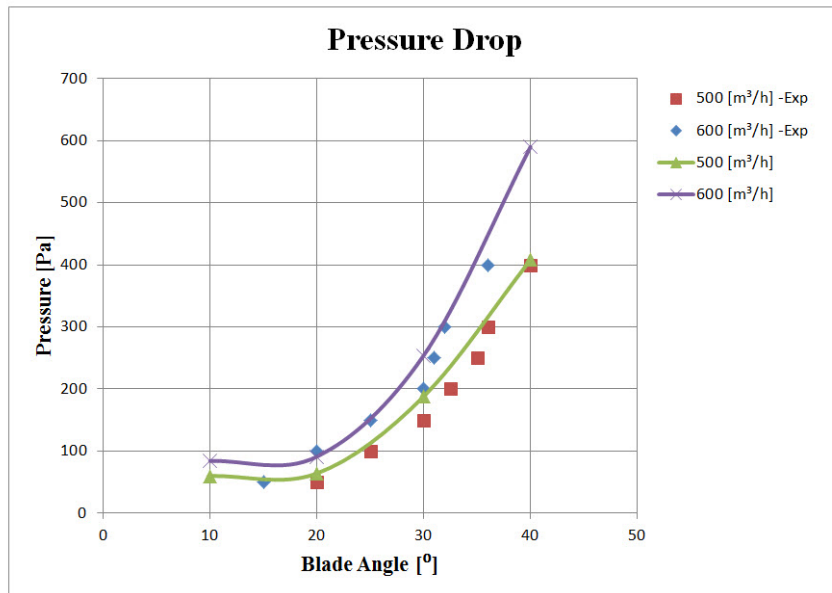


Figure 5.1: Pressure Comparison Between Experiment Results and CFD Results

Moment values on the 160 mm CAV unit blade is given in Figure 5.2. Experimental

results, CFD results and moment due to spring force is compared. Results are very close to each other.

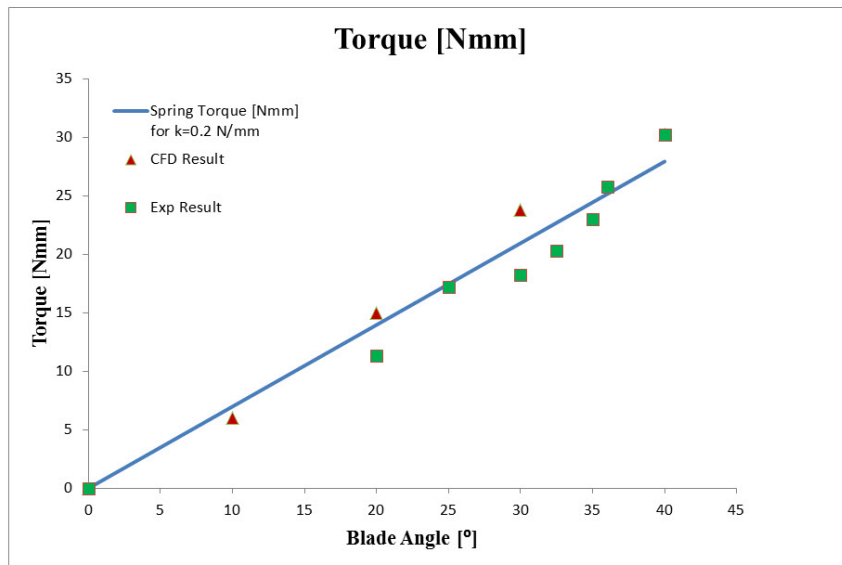


Figure 5.2: Moment Comparison Between Experimental Results, CFD Results and Spring Moment

In Figure 5.3. pressure drop over CAV unit is compared with experimental results, CFD results and theoretical results. Experimental results and CFD results are close to each other. Theoretical results are close to experimental results for small blade angles but under predicts pressure drop values especially for high blade angle. The reason is that theoretical model is constructed for 2D CAV unit and does not accurately model highly turbulent region after the blade. The difference increases with increasing blade angle.

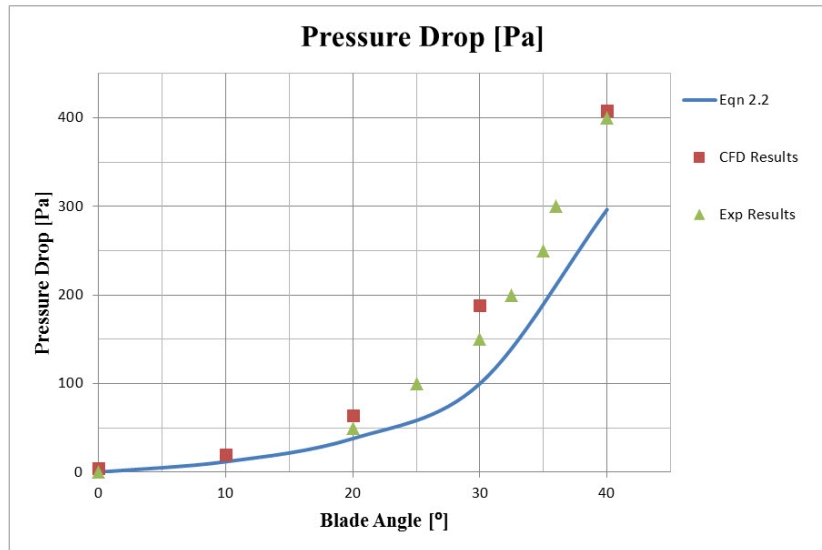


Figure 5.3: Pressure Drop Comparison Between Experimental Results, CFD Results and Theoretical Results

In this thesis, constant air volume device (CAV unit) for HVAC systems is designed. Moreover, CAV unit is tested by laboratory experiments and CFD analyses are validated according to these test results.

Design procedure starts with benchmark test. Commercially available CAV units are examined. This helps to understand the physics of the device. Then, experimental setup design process is started. By following some standards and methods test setup is designed. Robustness of the test setup is the main concern. Air leakage is also another problem and it increases system uncertainties. Since the amount of leakage cannot be measured, exact air flow rate cannot be known. Air leakage is tried to be minimized by applying silicone and sponge strips to the air ducts of setup which is explained in Chapter 4. In Figure 4.5 flow meter can be seen. This flow meter is tightly mounted to measurement setup to get most possible reliable results. Assembling the CAV unit to the experiment setup is also a critical part. For high flow rates, CAV unit is exposed to high drag force which may cause disengagement of the unit from test setup so it should be secured by means of safe strips. The setup can be seen in Figure 4.8. Bellows pressure is measured to see whether it inflates or not. For small blade angle vacuum is observed which means that bellow does not operate properly at fully open blade position. However, at these positions oscillations have low amplitude and easily

dampen out by friction on the system so it does not create a problem.

In this study, one of the CAV unit is manufactured from Plexiglas in order to see blade motion and air flow path as seen in Figure 5.4.

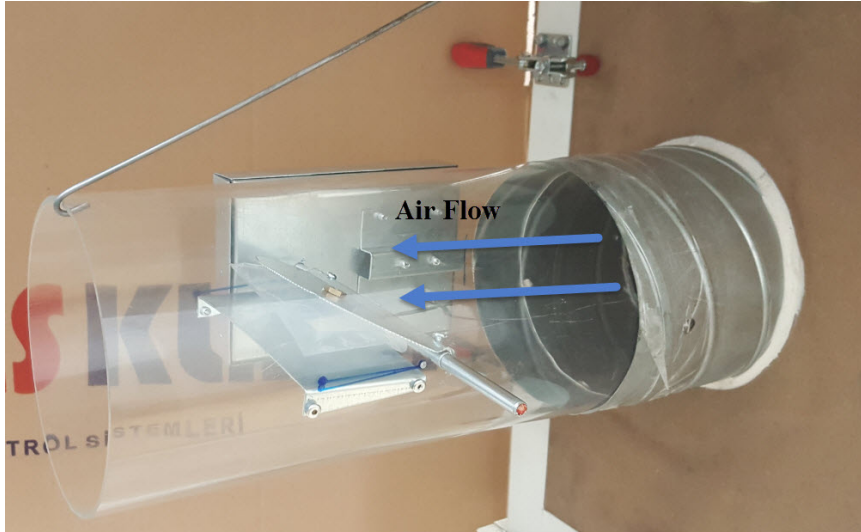


Figure 5.4: Plexiglass CAV Unit

In order to observe flow path, a flow visualization method is tried. By using smoke machine which is ECO FOGGER, smoke is supplied to the test setup which is shown in Figure 4.2 from left side of the fan unit. However, expected results cannot be obtained because of turbulent air flow. High flow rate creates turbulence inside air ducts and disturbs smoke flow. Moreover, smoke machine and CAV unit are away from each other so it is not possible to maintain laminar flow until CAV unit. This is the other reason for failing to observe flow path inside the CAV unit.

Experimental setup design takes most of the time which is spent for this thesis. Literature and HVAC standards are carefully examined before starting experiments. Pressure measurements are performed by following a HVAC standard which is stated in Chapter 4. In order to determine bellows pressure, experimental setup which has two manometers is designed. Torque on the blade is measured by load cell. Spring stiffness of tension springs are measured by different test setup but the same load cell. Air flow rate at the exit plane of CAV unit is also determined by hot wire anemometer. The main purpose is that if the air velocity at the exit plane is constant over time, the air flow rate is also constant. This measurement is mostly performed for finished

CAV units as a performance check. The photo of the final version of CAV unit can be found at appendix.

## **5.2 Conclusion**

Designed CAV unit is tested according to design criteria namely air flow rate accuracy and operating differential pressure range. Performance results of Ø160 mm diameter CAV unit are presented in Appendix A. Both of these CAV units are tested from 50 Pa to 700 Pa differential pressure and air flow velocity between 2 m/s to 10 m/s.  $\pm 10\%$  air flow rate range is also presented in all the performance result figures. As seen in the figures in Appendix A. Ø160 mm diameter CAV unit perfectly satisfies the project needs.

Both experimental and CFD results for pressure differential values are compared as seen in Figure 5.1. Both results almost give the same values. However, there are some differences between CFD results and experimental results. Numerical errors, modeling errors, uncertainty in measurements can be shown as the main reasons for differences. CAV unit operates in complex flow patterns and highly turbulent environment especially at the downstream region. Therefore, as a future work transient CFD solution with different turbulence models might be utilized to increase agreement in experimental and numerical results.



## REFERENCES

- [1] J. Taylor, B. Sinopoli, and W. Messner, “Nonlinear modeling of butterfly valves and flow rate control using the Circle Criterion Bode plot,” *Am. Control Conf. (ACC), 2010*, pp. 1967–1972, 2010.
- [2] W. T. Grondzik, *Air-Conditioning System Design Manual*, 2nd ed. Burlington, MA: Butterworth-Heinemann, 2007.
- [3] S. M. Gheji, K. S. Kamble, A. A. Gavde, and S. P. Mane, “Basic Classification of HVAC Systems for Selection Guide,” *Int. Journal Innov. Res. Sci. Engineering Technol.*, vol. 5, no. 4, pp. 6077–6086, 2016.
- [4] W. G. Gupton, *HVAC Controls*, 1st ed. The Fairmont Press Inc., 2002, vol. 1.
- [5] “VAV and CAV Systems,” 2017. [Online]. Available: <http://www.pricetwa.co.uk/products/vav-and-cav-systems>
- [6] “Cav-sabit hava debili sistemler,” no. 38. Alarko Carrier, May 2012.
- [7] A. Ş. Üçer, *Turbomachinery*, 1st ed. Ankara: METU, 1982.
- [8] Application considerations and estimated savings for vfd drives. [Online]. Available: <http://www.nrcan.gc.ca/energy/products/reference/15385>
- [9] T. Report, “Venturi Air Valve or Single-Blade Damper What ’s Right for You ?” no. 149, pp. 1–8, 2008.
- [10] E. Nishizu, M. Okubo, and E. Wada, “Automatic controlling device for maintaining a constant rate of air flow in air-conditioning equipment,” May 25 1976, uS Patent 3,958,605. [Online]. Available: <https://www.google.com.tr/patents/US3958605>

- [11] W. Finkelstein, G. Baumeister, and J. Haaz, "Regulator valve," Nov. 27 1979, uS Patent 4,175,583. [Online]. Available: <https://www.google.com.tr/patents/US4175583>
- [12] D. C. Leutwyler, Z., "A computational study of torque and forces due to compressible flow on a butterfly valve disk in mid-stroke position," *J. Fluids Engineering*, vol. 5, no. 128, pp. 1074–1082, 2006.
- [13] D. J. C. Morris, M. J., "An experimental investigation of butterfly valve performance downstream of an elbow," *Journal of Fluids Engineering*, vol. 113, no. 81, 1991.
- [14] A. D. Henderson, J. E. Sargison, G. J. Walker, and J. Haynes, "A Numerical Study of the Flow Through a Safety Butterfly Valve in a Hydro-Electric Power Scheme," *16th Australas. FluidMechanics Conf.*, vol. 3, no. December, pp. 1116–1122, 2007.
- [15] T. Sarpkaya, "Torque and cavitation characteristics of butterfly valves," *ASME*, p. 518, 1961.
- [16] T. T. F. K. Kimura, T. and K. Ogawa, "Hydrodynamic characteristics of a butterfly valve - prediction of pressure loss characteristics," *ISA Trans.*, vol. 4, no. 34, pp. 319–326, 1995.
- [17] M. Sandalci, E. Mançuhan, E. Alpman, and K. Küçükada, "Effect of the Flow Conditions and Valve Size on Butterfly Valve Performance," *Isi Bilim. Ve Tek. Dergisi/ J. Therm. Sci. Technol.*, vol. 30, no. 2, pp. 103–112, 2010.
- [18] M. H. Aksel, *Fluid Mechanics*, 3rd ed. Ankara: METU, 2011, vol. 1.
- [19] T. Sarpkaya, "Oblique impact of a bounded stream," *Journal of the Franklin Institute*, vol. 267, no. 3, pp. 229–242, 1959.
- [20] *Fluent Theory Guide*. Ansys Inc., 2018.
- [21] J. Srebric and Q. Chen, "An example of verification, validation, and reporting of indoor environment CFD analyses BT - ASHRAE Transactions 2002, June 22, 2002 - June 26, 2002," vol. 108 PART 2, no. 2, pp. 185–194, 2002.



- [22] A. D. Toro, “Computational Fluid Dynamics Analysis of Butterfly Valve,” vol. Utah State, 2012.
- [23] Puls Electronic, “FSM-2 Digital Weight Indicator Manual,” pp. 74–75.
- [24] TSI, “Air Flow ProHood Flow Meter Manual.”
- [25] Testo, “Testo 510 Differential Pressure Meter Manual.”
- [26] I. Extech, “Hot Wire Thermo-Anemometer with Datalogger.” [Online]. Available: <http://www.extech.com/resources/SDL350{ }UM-en.pdf>
- [27] J. S. Maurice, “Practise for measurement, testing, adjusting and balancing of building heating, ventilation, air-conditioning, and refrigeration systems,” *American Society of Heating, Refrigerating and Air-Conditioning Engineers, Inc*, no. 111, p. 24, 1988.
- [28] M. J. Suppo, W. D. Bevirt, R. J. Lavendar, C. N. Lawson, B. R. Meyer, A. H. Quinby, B. W. Engen, D. G. Virgin, F. L. Brown, D. R. Conover, C. E. Dorgan, E. C. Dowless, R. M. Martin, J. E. Sjoldal, and A. G. Wilson, “ASHRAE STANDARD Practices for Measurement , Testing , Adjusting , and Balancing of Building Heating , Ventilation ,,” 1988.



## APPENDIX A

### PERFORMANCE EVALUATION OF Ø160 MM CAV UNIT

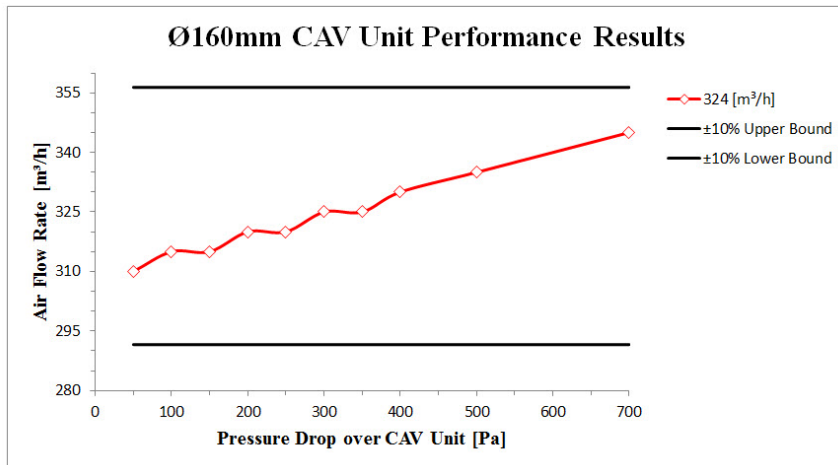


Figure A.1: Ø160 mm CAV Unit Performance Result for 324 m<sup>3</sup>/h

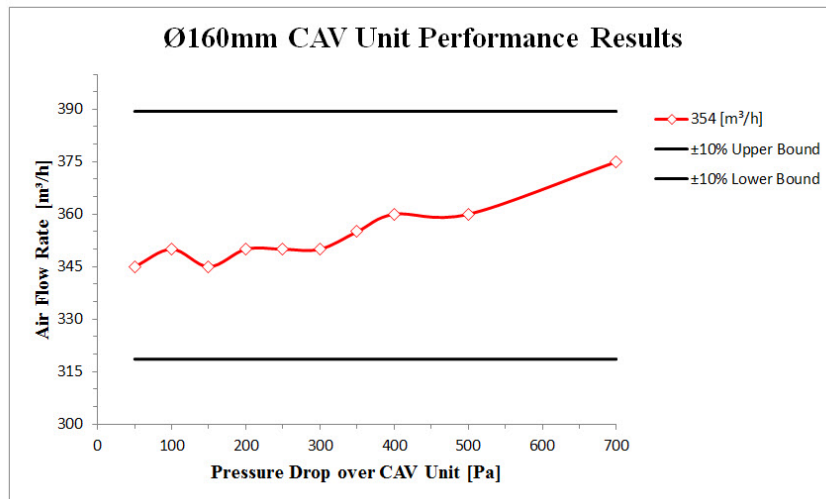


Figure A.2: Ø160 mm CAV Unit Performance Result for 354 m<sup>3</sup>/h

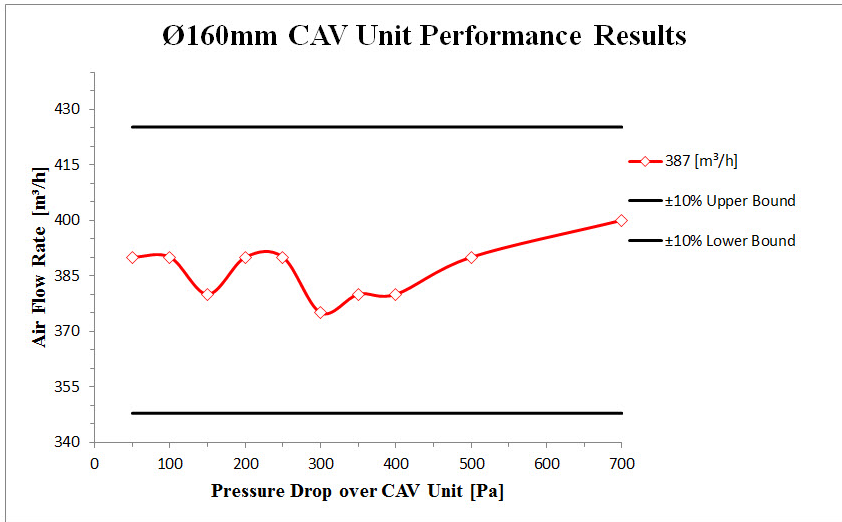


Figure A.3: Ø160 mm CAV Unit Performance Result for 387 m<sup>3</sup>/h

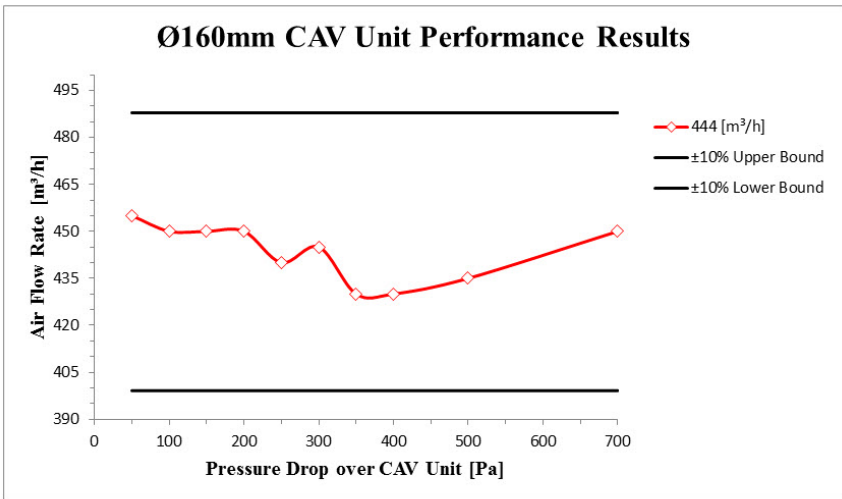


Figure A.4: Ø160 mm CAV Unit Performance Result for 444 m<sup>3</sup>/h

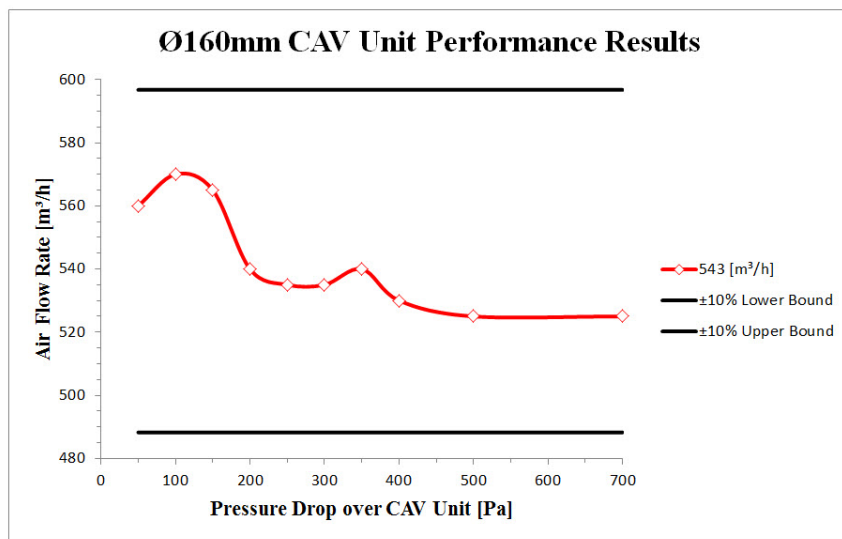


Figure A.5: Ø160 mm CAV Unit Performance Result for 543 m<sup>3</sup>/h



## APPENDIX B

### FINAL VERSION OF CAV UNIT

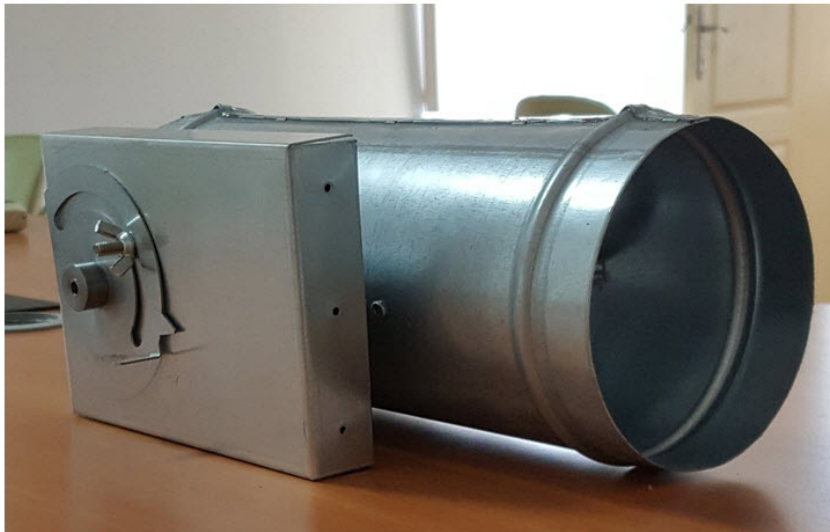


Figure B.1: Final Version of Circular CAV Unit